

CHARLES UNIVERSITY

FACULTY OF PHARMACY IN HRADEC KRÁLOVÉ

DEPARTMENT OF PHARMACEUTICAL CHEMISTRY AND
PHARMACEUTICAL ANALYSIS

UNIVERSITY OF LJUBLJANA

FACULTY OF PHARMACY

DEPARTMENT OF PHARMACEUTICAL CHEMISTRY

**Synthesis and evaluation of probes for fluorescent
microscopy based on cyanopyridines and merocyanine
scaffolds and lanthanide complexes**

Diploma thesis

Supervisors: PharmDr. Marta Kučerová, Ph.D.

Consultant: Assist. prof. Stane Pajk, M. Pharm., Ph.D.

Juraj Bajnok

ERASMUS Project

2022

DECLARATION

"I declare that this thesis is my original author's work, which has been composed solely by myself (under the guidance of my consultant). All the literature and other resources from which I drew information are cited in the list of used literature and are quoted in the paper. The work has not been used to get another or the same title. "

Juraj Bajnok

Hradec Králové, August 2022

ACKNOWLEDGEMENT

I would like to thank to PharmDr. Marta Kučerová, Ph.D. for her help and practical advice in the lab, for her support, when I decided to go on the Erasmus project, and for time spent on correcting my diploma thesis.

My gratitude goes to Assist. prof. Stane Pajk, M. Pharm., Ph.D., who supervised my work in the lab, for his great support, for his friendly approach to students, for showing me how to solve problems in the lab, and for all his experience he shared with me.

I would like to thank to Aljoša Bolje Ph.D. for the time spent in the lab with me, for his advice, and for everything I have learnt from him.

I also want to thank everyone, who participated somehow in keeping good mood in the lab or helped me with either lab work or diploma thesis writing.

ABSTRACT

Charles University

Faculty of Pharmacy in Hradec Králové

Department of Pharmaceutical Chemistry and Pharmaceutical Analysis

Student: Juraj Bajnok

Supervisor: PharmDr. Marta Kučerová, Ph.D.

Consultant: Assist. prof. Stane Pajk, M. Pharm., Ph.D.

Title of diploma thesis: Synthesis and evaluation of probes for fluorescent microscopy based on cyanopyridines and merocyanine scaffolds and lanthanide complexes

Fluorescence as part of luminescence is a process, which describes how electrons of suitable materials are excited by the energy absorption of a photon, followed by the immediate emission of a photon with less energy compared to the absorbed photon. Suitable compounds must contain a system of conjugated double bonds.

In this thesis, we present the synthesis and evaluation of fluorescence on derivatives of cyanopyridines, merocyanine-type fluorescent probes, and lanthanide complexes of terbium, dysprosium, and europium. Lanthanide ions have low molar extinction coefficients, therefore they cannot be excited directly, without a proper ligand. We explored the influence of pH on the emission of synthesized derivatives of cyanopyridines. We synthesized two merocyanine dyes with new alkyl moieties, which should change their emission spectra. Then, the merocyanine dyes could serve as new fluorescent probes for labelling lipid droplets.

Our idea was preparation of several lanthanide complexes with ligands containing clickable structural moieties. Click chemistry is a simple, fast procedure, which can produce 1,4-disubstituted triazoles. Lanthanide complexes with substituted triazoles performed strong fluorescence because of their even bigger system of conjugated double bonds.

ABSTRAKT

Univerzita Karlova

Farmaceutická fakulta v Hradci Králové

Katedra farmaceutické chemie a farmaceutické analýzy

Student: Juraj Bajnok

Školitel: PharmDr. Marta Kučerová, Ph.D.

Konzultant: Assist. prof. Stane Pajk, M. Pharm., Ph.D.

Název diplomové práce: Syntéza a hodnocení sond pro fluorescenční mikroskopii založených na kyanopyridinových a merocyaninových derivátech a lanthanoidových komplexech

Fluorescence jako součást luminiscence je proces, při kterém se elektrony molekul excitují, čímž se dostávají na vyšší energetickou hladinu díky absorpci energie fotonu. Následně elektrony vyzařují foton o nižší energii, čímž se vrátí zpět na nižší energetickou hladinu. Aby byla látka schopná vykazovat fluorescenci, musí obsahovat konjugovaný systém dvojných vazeb.

V této práci představujeme syntézu a hodnocení fluorescence látek založených na derivátech merocyaninového a kyanopyridinové strukturního typu a komplexech s vybranými lanthanoidy, jako je terbium, europium a dysprosium. Lanthanoidové ionty nemohou být excitované přímo bez vhodného ligandu, což je způsobeno jejich nízkým molárním extinkčním koeficientem. Po syntéze kyanopyridinových derivátů jsme měřili vliv pH prostředí na jejich výsledná emisní spektra. Naším dalším cílem byla syntéza merocyaninových barviv s novými alkylovými substituenty ve struktuře se snahou obměnit jejich výsledná emisní spektra tak, aby látky mohly sloužit jako nové fluorescenční sondy pro označování lipidových kapiček.

Poslední částí mé práce byla příprava lanthanoidových komplexů s ligandy, které ve své struktuře obsahují prvky umožňující "click" reakci, což je jednoduchý proces, při kterém dochází k vytvoření 1,4-disubstituovaných triazolů. Lanthanoidové komplexy obsahující navázané triazoly jsou schopné jasné fluorescence díky delšímu systému konjugovaných dvojitých vazeb.

Contents

1	Abbreviations	8
2	The aim of the diploma thesis	10
3	Theoretical part	12
3.1	Fluorescence and phosphorescence	12
3.2	The Stokes Shift.....	13
3.3	Basic characteristics of a fluorophore	14
3.3.1	Fluorescence quenching	16
3.4	Fluorophores.....	17
3.4.1	Labelling of lipid droplets	18
3.4.2	Lanthanides as fluorophores.....	19
3.4.3	Europium, Dysprosium, Erbium, Terbium.....	21
3.4.4	Lanthanides as thermometers	21
3.5	Click chemistry.....	23
3.5.1	Classification of CCh	23
3.5.2	Cycloadditions.....	24
3.5.3	The use of Click chemistry.....	25
4	Experimental part	27
4.1	Materials, instruments, analytical methods	27
4.2	Synthesis of nitrogen bridgehead fused cyanopyridines	28
4.2.1	Synthesis of compound 1 and 2	28
4.2.2	Synthesis of compound 3 and 4	29
4.3	Synthesis of merocyanine-type fluorescent probes for labelling lipid droplets.....	30
4.3.1	Synthesis of compound 5 , 6 , 7 , 8 and 9	30
4.3.2	Synthesis of compound 10 , 11 , 12 , 13 , 14 , 15 , 16 and 17	33
4.4	Ligands	39
4.4.1	Synthesis of ligand 20	39

4.4.2	Synthesis of ligand 21	41
4.4.3	Synthesis of compound 22	41
4.5	Click reactions with lanthanide complexes	42
4.5.1	Synthesis of lanthanide complexes	42
4.5.2	Click chemistry with lanthanide complex	45
5	Results and discussion	49
6	Conclusion	59
7	References	60

1 Abbreviations

AAC – azide-alkyne cycloadditions

ACN – acetonitrile

calcd - calculated

CCh – click chemistry

CuAAC – Cu(I)-catalyzed azide-alkyne cycloadditions

DCM – dichloromethane

DMAP – *N,N*-dimethylpyridin-4-amine

DMF – dimethylformamide

DMSO – dimethylsulfoxide

DQ – dynamic quenching

EFB – ethyl 4,4,4-trifluoro-3-oxobutanoate

equiv – equivalent

EtOAc – ethyl acetate

Et₂N – diethylamine

Et₃N – triethylamine

FAD – flavin adenine dinucleotide

Hex – hexane

IC – internal conversion

JD – Jablonski diagram

LDs – lipid droplets

LI – lanthanide ion

LLs – luminescent lanthanide labels

MeOH – methanol

NAD – nicotinamide adenine dinucleotide

NIR – near-infrared

NMR – nuclear magnetic resonance

PL – photoluminescence

PROTACs – proteolysis-targeting chimeras

RT – room temperature

S₀ – singlet ground electron state

S₁ – singlet first electron state

S₂ – singlet second electron state

SQ – static quenching

SS – Stokes shift

TLC – thin layer chromatography

TRF – time-resolved fluorescence

UV – ultraviolet light

2 The aim of the diploma thesis

My diploma thesis' aim was the synthesis of three types of organic compounds with a conjugated system of double bonds.

Fluorescent nitrogen bridgehead fused cyanopyridines were discovered as a side product when the reaction between 2-cyanothioacetamide and chloroacetone was left to react for a week (**Figure 1**) [1]. In this thesis, we planned to synthesize several derivatives and test the influence of pH on their emission spectra.

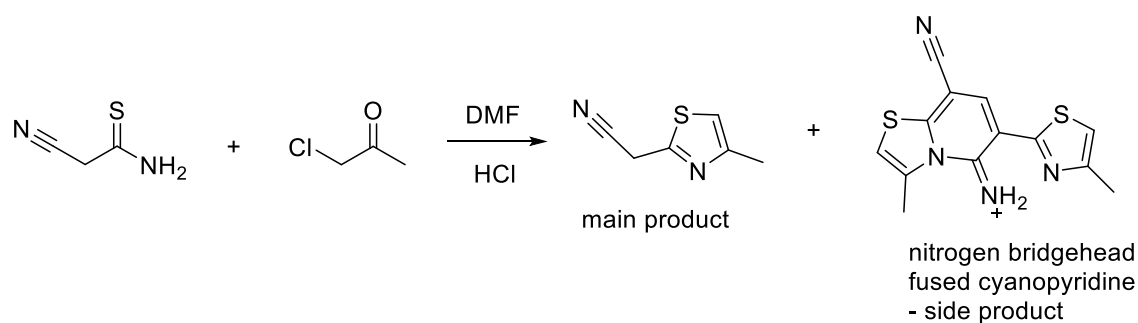


Figure 1: Synthesis of cyanopyridines

Another goal was the synthesis of two derivatives of the merocyanine dye (**Figure 2**) by substitution of diethylamino moiety (in red) of a successful lipid droplet label synthesized previously with alkyloxy substitution (blue) or by condensation with 1,2,2,4-tetramethylpyridine (green) [2]. We hoped the introduced moieties would change excitation and emission spectra and thus provide new tools for labeling lipid droplets.

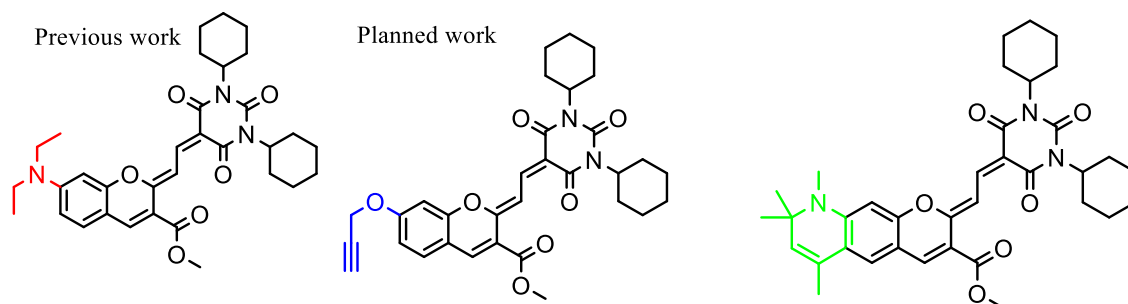


Figure 2: Synthesized merocyanine dyes

Many known ligands form bright complexes with europium and terbium, however, their further functionalization limits their usefulness. In this thesis, we intended to synthesize new ligands with “clickable” groups that would enable further derivatization. From ligands, we planned to synthesize complexes and evaluate their emission. Selected complexes would be reacting with silyl reagent to form probes for

labeling glass surfaces. These probes were intended as ratiometric temperature sensors.

3 Theoretical part

3.1 Fluorescence and phosphorescence

Fluorescence describes the phenomenon that starts with the absorption of a photon by an excitable material, followed by the emission of a photon with less energy compared to the photon that was absorbed. That means that emitted light will have a longer wavelength compared to absorbed one since light with a shorter wavelength has higher energy in comparison to light with a longer wavelength [3]. Chemical molecules that exhibit fluorescent properties are called fluorophores. Following absorption of a photon, electrons move from the ground singlet state to the excited singlet state, which is typical for fluorescence. This is different compared with phosphorescence, where the movement to the higher energy state is accompanied by a change in spin and thus the electron is in a triplet excited state. In both cases, i.e., fluorescence and phosphorescence, excited electrons return to the ground state by emitting a photon. The whole process is best depicted with the Jablonski diagram (JD) shown in **Figure 3**.

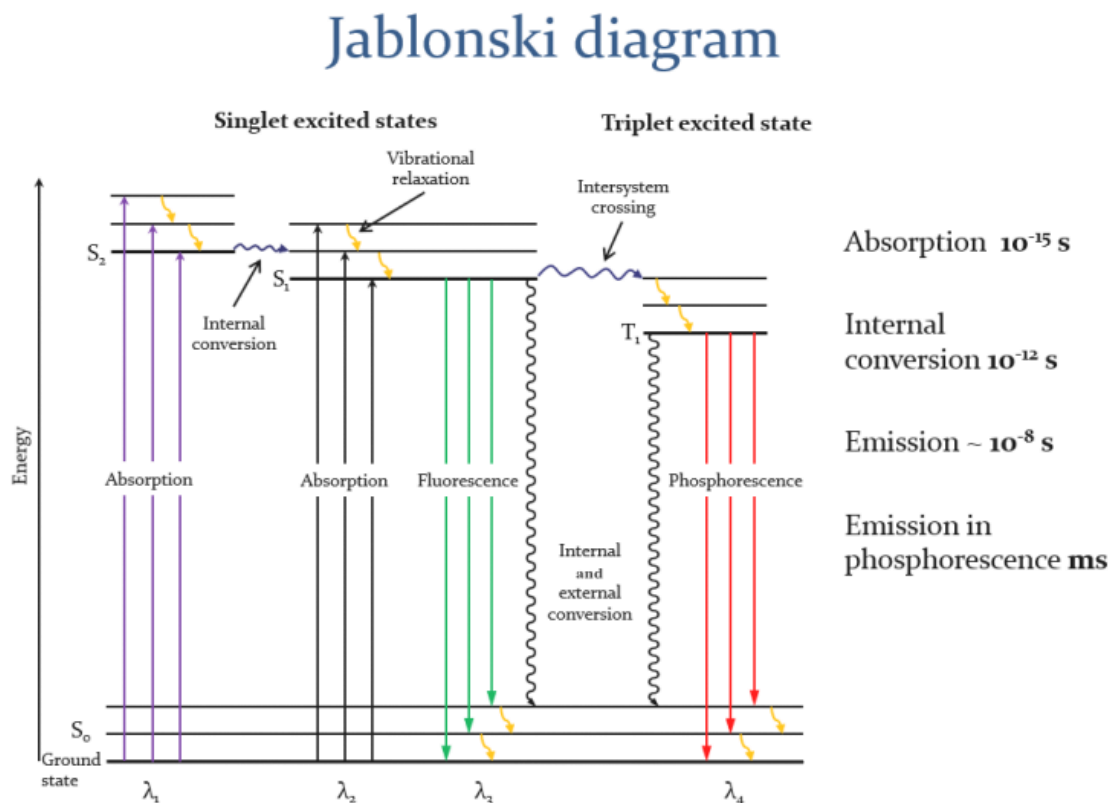


Figure 3: Jablonski diagram, copied from Pajk, S. [2]

Electron transitions occur between energy levels represented by horizontal lines in the Jablonski diagram (JD), the vertical lines illustrate transitions between different energy

levels. Besides the ground state (S_0), the state with the lower energy, there are several excited states (S_1, S_2). Additionally, these states have many vibrational levels. An excited electron can occupy any of the possible vibrational levels of the excited state. If the electron following absorption occupies the S_2 state, it rapidly undergoes internal conversion (IC) to S_1 . Internal conversion is a prompt process, which takes roughly 10^{-12} s, compared to fluorescence, which occurs in 10^{-8} s, so IC is completed by the time when emission occurs, and we seldom observe the emission from S_2 . The electron then undergoes vibrational relaxation to the lowest vibrational level of the excited state, from where it relaxes to one of the vibrational levels of the ground state by emission of a photon [4].

The average time that the fluorophore remains excited is referred to fluorescence lifetime, for organic fluorophores they are typically between 1 to 10 ns [5]. On the other hand in the case of phosphorescence, the lifetimes are in the order of ms, because the transition from the excited triplet state to the singlet ground state is formally forbidden [6].

3.2 The Stokes Shift

The Stokes shift (SS) belongs to the basic characteristics of fluorescence. Jablonski's diagram reveals that the energy of absorption exceeds the energy of emission. Fluorescence emission is therefore observed at longer wavelengths compared to excitation. It has its name after Sir G. G. Stokes, who was the first one to observe this effect (**Figure 4**). There was an early experiment, in which quinine absorbed light from the sun. This light was transmitted at a wavelength less than 400 nm through blue glass, that served as a filter. It is common knowledge now, that quinine emits light close to 450 nm and so makes its fluorescence visible. JD shows that there is an energy loss between absorption and emission. One cause is vibrational relaxation to the lowest vibrational level of S_1 . Considering that fluorophores usually decay to the higher vibrational level of S_0 , we can expect even greater losses of excitation energy. The latter also means that the shape of the emission spectra (but not the intensity) is going to be independent of excitation wavelength because the emission is going to be observed only from the lowest vibrational level of S_1 [7].

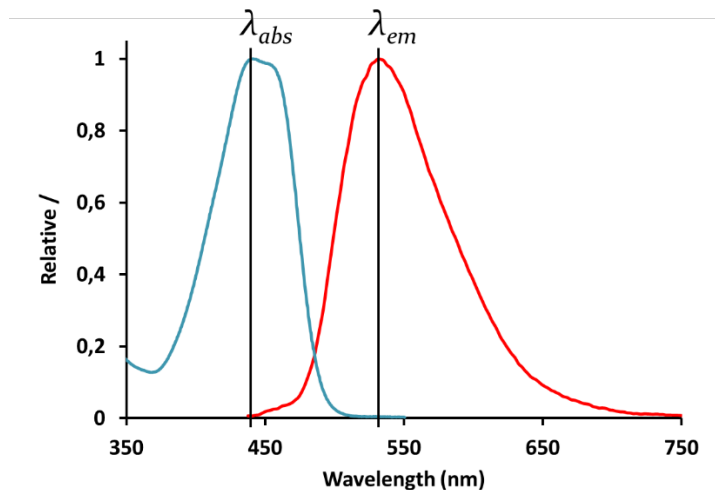


Figure 4: Typical absorption (blue) and emission (red) of an organic fluorophore. Stokes shift represents the difference between positions of maximal absorption (λ_{abs}) and maximal emission (λ_{em}). This figure was copied from Pajk, S. [2]

3.3 Basic characteristics of a fluorophore

Fluorescence quantum yield and lifetime belong to the most crucial properties of fluorophores. Fluorescence quantum yield ϕ_f represents the number of emitted photons compared to the number of absorbed photons. Quantum yield can be represented also as a ratio between the radiative rate constant k_r and the sum of radiative k_r and nonradiative rate k_{nr} constants (**Equation 1**).

$$\phi_f = \frac{k_r}{k_r + k_{nr}}$$

Equation 1: calculation of quantum yield

The latter one includes all possible processes of decay without emission. Even though we cannot achieve the complete quantum yield of a defined fluorophore, we can modulate the structure of a fluorophore to get better results. For example, increased rigidity of the structure of a fluorophore minimalizes vibrations or rotations of functional groups which can cause before mentioned nonradiative deactivation (**Figure 5**) [8].

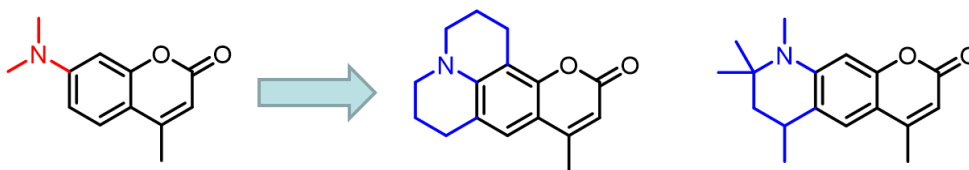


Figure 5: Example of introduction of rigidity in the structure 7-(dimethylamino)-4-methyl-2H-chromen-2-one; dimethylamino group (highlighted in red) is substituted with more rigid aliphatic heterocycles (blue). This figure was copied from Pajk, S. [2]

Fluorescence lifetime τ_f specifies the average time of a molecule in its excited state before it returns to the ground state. It can be calculated according to **equation 2**. The fluorescence lifetime for organic fluorophores is usually between 1 to 10 ns (**Figure 6**). Intrinsic or natural lifetime defines a lifetime without nonradiative processes. **Equation 3** provides the calculation of τ_n [7,9].

$$\tau_f = \frac{1}{k_r + k_{nr}}$$

Equation 2: calculation of fluorescence lifetime

$$\tau_n = \frac{1}{k_r}$$

Equation 3: calculation of natural lifetime

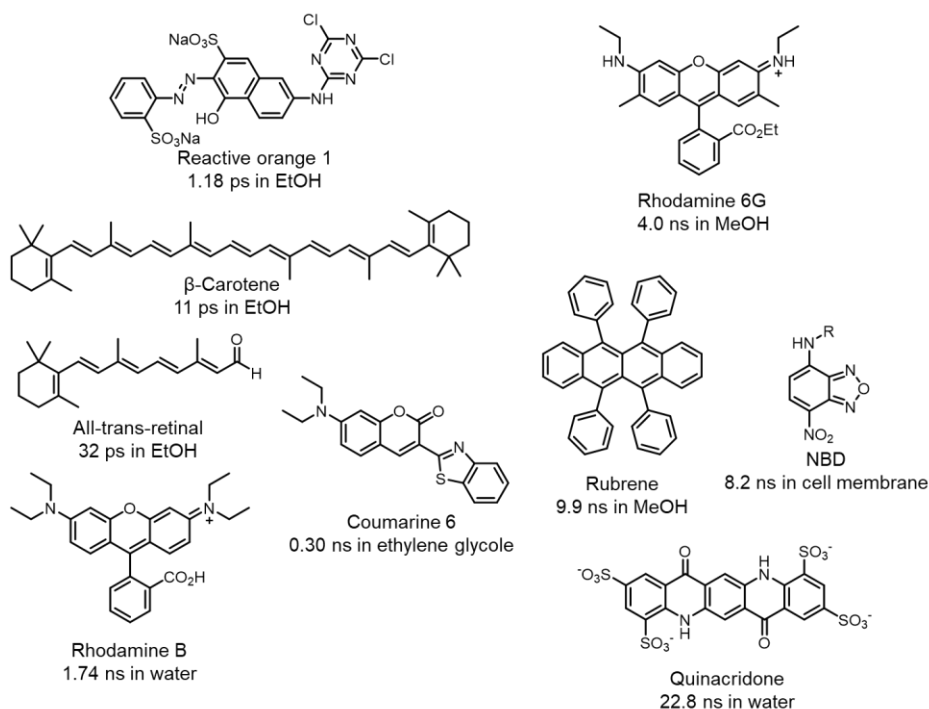


Figure 6: Examples of fluorophores with their respective fluorescence lifetimes. The rigidity of the structure increases the fluorescence lifetime. Note the typical short fluorescence lifetime of the naturally occurring β -carotene and all-trans-retinal. This figure was copied from Pajk, S. [2]

3.3.1 Fluorescence quenching

A fluorophore in its excited state can interact with ions and molecules in solution, which may result in the transition of a fluorophore from an excited state to the ground state without the emission of a photon. This process of reducing the intensity of fluorescence is called quenching and regarding the mechanism we can further divide it into dynamic or collisional quenching (DQ) and static quenching (SQ).

In DQ the molecule causing the quenching is called a quencher. Stern-Volmer equation (**Equation 4**) describes the process of DQ, where k is the Stern-Volmer quenching constant, k_q represents bimolecular quenching constant, t_0 indicates unquenched lifetime and $|Q|$ is the concentration of quencher. The value of k indicates how sensitive is a fluorophore toward the quencher. This constant can reach both high and low values depending on the environment in the solution. If a fluorophore is free in solution, then the constant is high. On the other hand, if fluorophore is hidden deep inside a biomolecule, the value of the Stern-Volmer quenching constant is low. Some examples of collisional quenchers are amines, halogens, oxygen, and electron-deficient molecules.

$$\frac{F_0}{F} = 1 + k|Q| = 1 + k_q t_0 |Q|$$

Equation 4: Stern-Volmer equation

In contrast to dynamic quenching, static quenching (SQ) occurs at the fundamental state of a complex. This complex of fluorophore and quencher is unable to emit photons. SQ is described by **equation 5**, where k_a represents the association constant, FQ is the concentration of a complex, F_1 represents the concentration of a fluorophore and Q_1 is the concentration of a quencher. An increasing concentration of the quencher does not change the lifetime of the fluorophore [10].

$$k_a = \frac{FQ}{F_1 Q_1}$$

Equation 5: calculation of static quenching

3.4 Fluorophores

There are many ways to classify fluorophores, by their origin we can distinguish intrinsic and extrinsic fluorophores. Intrinsic fluorophores are those, which are not man-made and are found in practically all living beings, from bacteria to more complex animals. An example is the indole group of amino acid tryptophan that absorbs light at 280 nm and emits at an emission maximum of 320 nm. Phenylalanine, NADH, FAD fluoresce similarly (**Figure 7**). Unfortunately, these intrinsic fluorophores are not useful in fluorescence microscopy and are responsible for the background fluorescence of the autofluorescence of the sample. Therefore, to visualize samples under the fluorescent microscope the samples are first labelled with fluorescent probes, i.e., extrinsic fluorophores (**Figure 8,9 and 10**) [7,11].

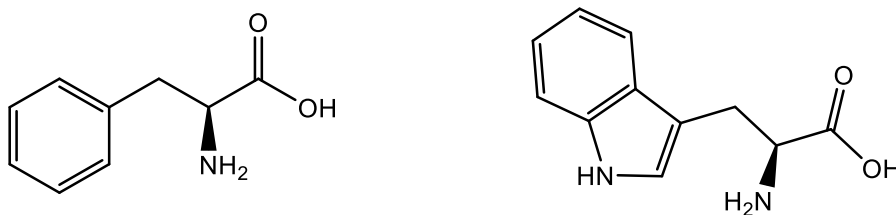


Figure 7: Examples of intrinsic fluorophores, phenylalanine (left) and tryptophan (right)

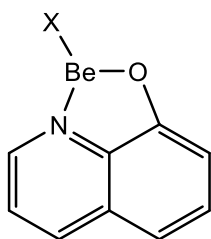


Figure 8: Metal chelate structure as an example of extrinsic fluorophore

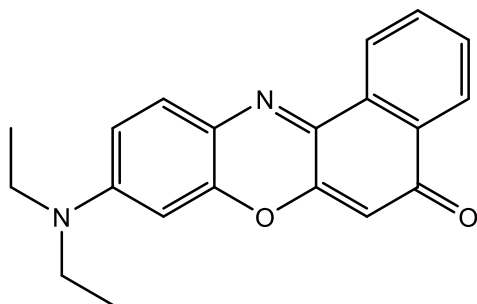


Figure 9: A Nile Red is a commonly used dye (extrinsic fluorophore)

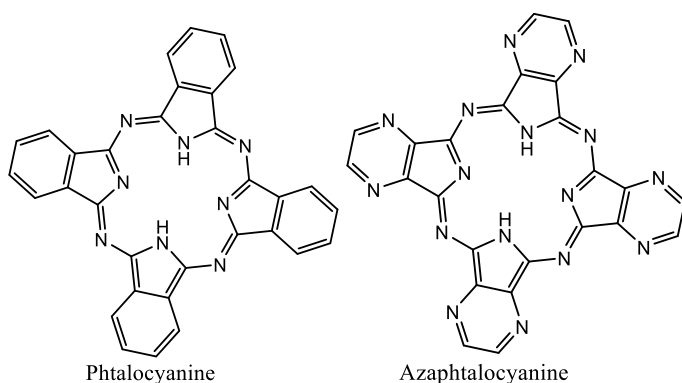


Figure 10: General formula of phtalocyanine and azaphtalocyanine as extrinsic fluorophores

3.4.1 Labelling of lipid droplets

One of the aims of my diploma thesis was the synthesis of merocyanine probes, that might be used as potential dyes for marking lipid droplets (LDs). LDs are cytosolic organelles, which are located in most eucaryotic organisms. They help to store fats as source of energy, and thus maintain energy homeostasis. Potential dye must be hydrophobic in order to move freely in non-polar environment of LDs. Nile Red (**Figure 9**) is commonly used lipophilic dye for LDs detection. Firstly, given dye in concentration of 1 mg/mL is added to 10 ml of 150 mM NaCl. Secondly, chosen cells are stained by 1 ml of dye, incubated for 10 minutes at room temperature, so the dye can accumulate in LDs. After incubation time, cells are washed three times with 2 mL of phosphate-buffered saline. Lastly, cells are analyzed with fluorescence microscopy [12-14].

3.4.2 Lanthanides as fluorophores

Lanthanides include fifteen elements starting from lanthanum up to lutetium. They represent the 6th period and III B group in the Periodic Table [15]. Luminescence based on lanthanides is different compared with the fluorescence of organic fluorophores. Emission spectra of luminescent lanthanide labels (LLs) originate in so-called “forbidden” f transitions. Direct excitation of these metals is almost impossible because of very low molar extinction coefficients (ϵ). LLs consist of a lanthanide ion (LI) and a ligand with good ϵ and are additionally capable of transferring the energy of a photon to the lanthanide. This is also called an antenna effect (**Figure 11**).

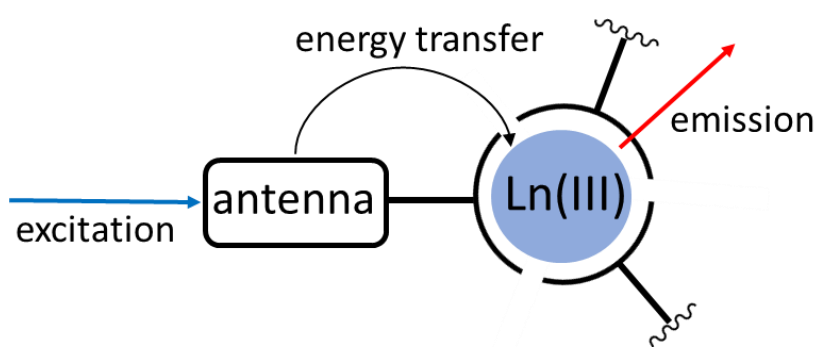


Figure 11: The antenna effect of lanthanide ion and ligand with good molar extinction coefficients. This figure was copied from Pajk, S. [2]

Besides improving the ϵ , ligands also play a key role in protection of LI from the environment. Usually, the common coordination number of lanthanides is 8 or 9. As an example, a typical Eu complex is formed by three bidentate ligands (commonly 1,3-diketones) and an auxiliary bidentate ligand (commonly phenanthroline), as it is shown in **Figure 12**. The first ones are responsible for increasing the ϵ and the latter ones are responsible for increasing quantum yield.

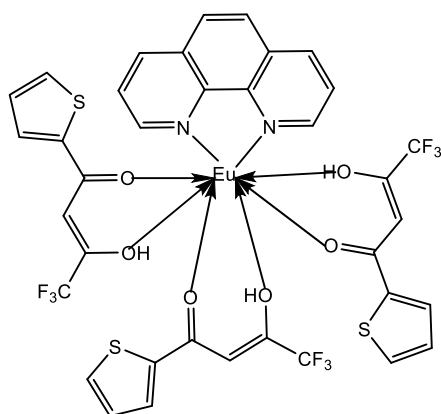


Figure 12: Example of a EuTTA3Phen complex

Stokes shifts are in hundreds of nanometers providing a clear separation of absorption and emission spectra. Additionally, the emission bands are narrow compared with the organic fluorophores. Another advantage of lanthanide complexes is their long lifetimes. For comparison, typical fluorescent molecules persist in their excited state in order of nanoseconds, whereas lanthanides stay excited in order of milliseconds. This is utilized in a biomedical application where the samples exhibit a lot of autofluorescence, however, fluorophores responsible for autofluorescence have a short fluorescence lifetime (**Figure 13**). Thus, following the excitation pulse, the signal from the lanthanide complex label is collected only after a lag time, when the signal from autofluorescence has already vanished. This increases the selectivity and sensitivity of the method.

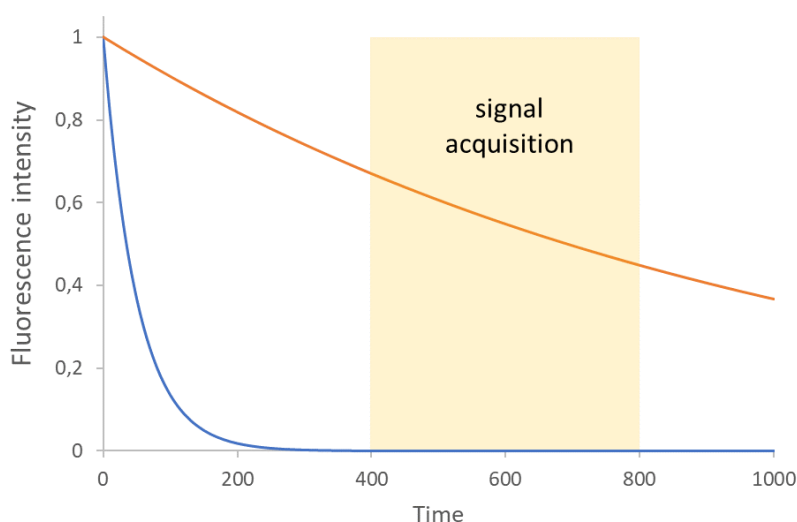


Figure 13: The difference between autofluorescence and fluorescence of lanthanide complex. The orange line represents a signal of the lanthanide complex, and the blue line represents a signal from autofluorescence. This figure was copied from Pajk, S. [2]

Even though the advantages of lanthanides are significant, yet they are limited by their brightness and excitation in UV region. They are also insensitive to the polarity of their environment because their excited state is protected by fully occupied $5s^2$ and $5p^6$ orbitals [16-20].

3.4.3 Europium, Dysprosium, Erbium, Terbium

Europium (Eu) is a rare metal-earth element, which belongs to the lanthanoid series of chemical elements. As a part of lanthanide chelates, it is in its trivalent ion form (Eu^{3+}). In form of chelates, Eu is capable of red photoluminescence (PL). Eu absorbs approximately from 300 to 400 nm. Emission peaks of Eu complexes are typically recorded around 580, 590, 610, and 650 nm. Emission spectra of Tb^{3+} complexes include four emission peaks, which are located around 490, 550, 580, and 620 nm. Complexes with Dy^{3+} are capable of emitting both near-infrared (NIR) and visible lights. As for all lanthanide complexes, also for europium complexes, long lifetimes in μs are typical. Complexes of europium are used to study cellular environments, e.g., they were used to examine phosphate receptors, nucleoside phosphate receptors, bicarbonate receptors, and many others. Depending on the desired emission wavelength other lanthanides may be used, such as terbium, erbium, dysprosium, and ytterbium [19,21-25]. The application of lanthanide complexes is wide and predestined by long-lived excited states of LI, especially Tb and Eu. Complexes with LIs produce intense bright fluorescence, which makes them appropriate material in biomedical and sensing fields or for water content determination, acetaldehyde detection, etc. Other LIs, such as dysprosium or erbium, emit in NIR region of light, which makes them promising agents for not only medical but telecommunication use, as well [26-31].

3.4.4 Lanthanides as thermometers

The emission of practically all fluorophores is dependent on the temperature, usually, emission decreases with increasing temperature, because of more collisions between the fluorophore and the molecules from its surrounding environment. However, this is rarely used to measure the temperature, since we do not know the exact concentration of the fluorophore. Fluorophores are also prone to photobleaching. One of the solutions is to use emission maxima with different temperature coefficients and use the ratio of emission (**Figure 14**). This way the changing concentration of the fluorophore does not influence the measurement. However, suitable organic fluorophores with such properties are difficult to find, on the other hand, some lanthanide complexes have relatively narrow

emission bands with different temperature coefficient, making them ideal for ratiometric thermometers. Thermal sensing is an essential method for understanding heat production in cells. Europium pyrazole complexes demonstrate an increase in luminescence intensity when heated over 200 °C. Overheating over certain temperature causes irreversible changes in enzymes, vaccines, chemicals, etc. Only a very sensitive marker can show the difference. Luminescent markers may be of choice, because of their non-invasiveness, low cytotoxicity, short transitory acquisition times, and high spatial and temperature resolutions. Properties, such as irreversible luminescence changes upon heating at a certain temperature, a high on/off ratio, a high luminescence intensity, and narrow luminescence bands with a constant position, are desirable for a suitable luminescent marker. Up-converting systems based on Er^{3+} , Yb^{3+} belong among such compounds. [32-37].

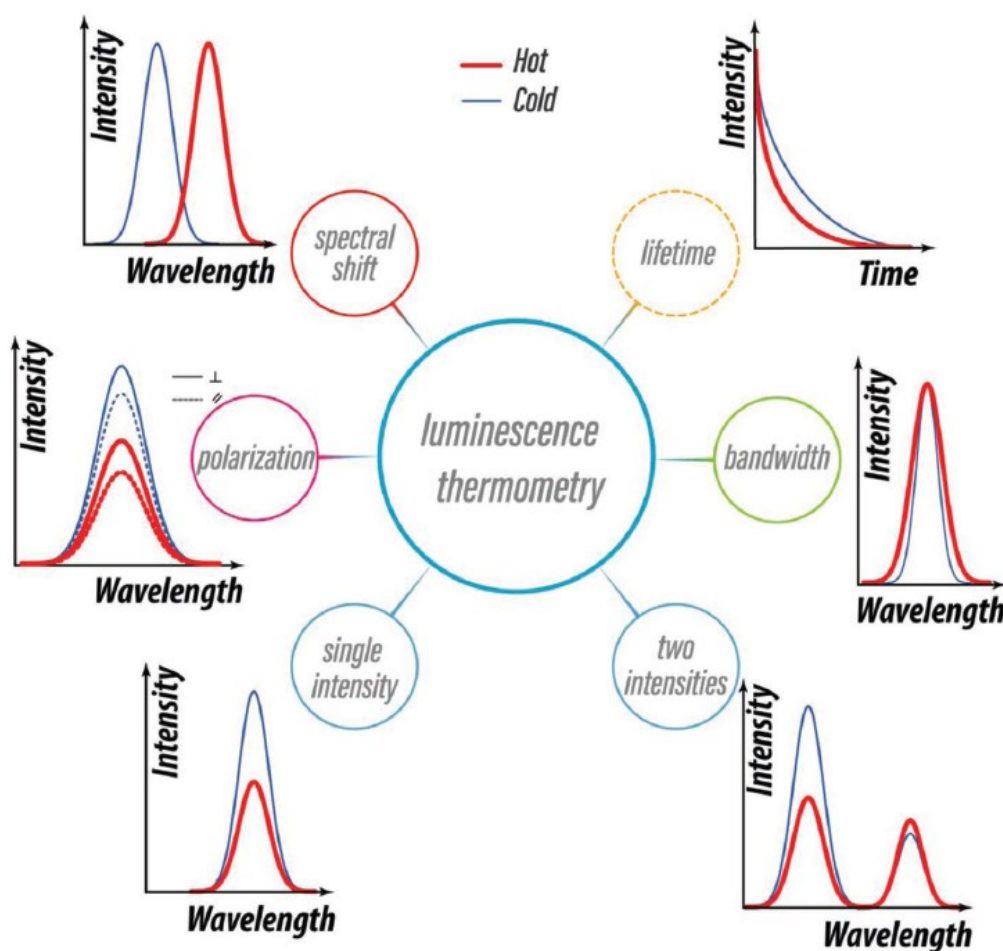


Figure 14: Some options of temperature measurement with luminescent material. This picture was copied from Pajk, S. [2]

3.5 Click chemistry

Click chemistry (CCh) is a set of reactions based on similar principles. The term “Click chemistry” was proposed by Sharpless et al. in 2001. To meet the criteria of CCh, the reaction should proceed under mild conditions and should be irreversible [38]. Additional conditions to classify a reaction as a click reaction are: reaction must be modular, wide in scope, stereospecific, give high yields, and produce little byproducts, which can be eliminated with non-chromatographic methods. The reaction conditions must also be simple (preferably, the reaction is insensitive to both water and oxygen), the reaction can be done in benign solvents (water) or without a solvent, starting material and all reagents must be easily available and the final product should be simply isolatable. A high thermodynamic driving force is typical for CCh. It is usually over 20 kcal/mol. Such a process proceeds quickly with high selectivity for a final product. This is the reason, why CCh is the procedure often used for the modification of lipids, proteins, and other molecules to label them with fluorophores, radioisotopes, or to form conjugates [39].

3.5.1 Classification of CCh

CCh comprises simple reactions with high yields, that produce an outcome in high purity and with high selectivity. Four main types of CCh can be distinguished:

1. Cycloadditions – include hetero-Diels-Alder reaction and mainly 1,3-dipolar cycloadditions [40].
2. Nucleophilic ring-openers – it means the opening of strained heterocyclic electrophiles [40].
3. Carbonyl chemistry of non-aldol type – formation of urea, thiourea, hydrazones, etc. is typical for this chemistry. Carbonyl chemistry of Aldol type on the other hand is not considered a CCh because of its low thermodynamic driving force, long reaction time, and variety of side products [40].
4. Additions to carbon-carbon multiple bonds – consist of dihydroxylations, epoxidations, aziridinations, etc. [40].

3.5.2 Cycloadditions

The first example of 1,3-dipolar cycloadditions dates to 1893. It was the reaction of terminal alkynes with organic azides, which afforded 1,2,3-triazoles. In the 1960s, Huisgen's investigations on azide-alkyne cycloadditions (AAC) provided a principle, which became a useful part of organic chemistry because of the simple preparation of starting materials. However, Huisgen's AAC has its limitations, such as long reaction time, high temperature and most importantly the formation of two regioisomers [41].

Sharpless and Meldal independently discovered that the addition of Cu(I) catalyst to a terminal alkyne and an organic azide in the presence of a weak base produces selectively 1,4-disubstituted triazoles in high yields. As a catalyst, practically any Cu(I) salt soluble in the solvent of the reaction mixture can be used (**Figure 15**).

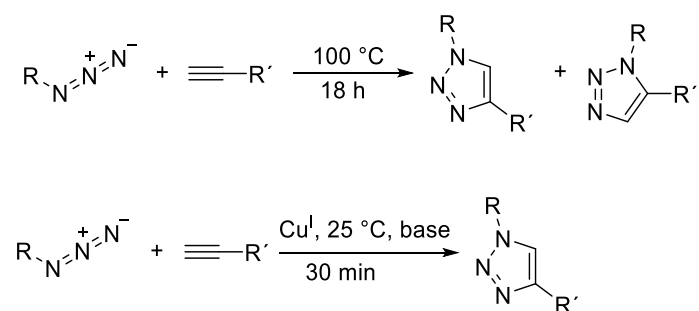


Figure 15: Difference between catalyzed and non-catalyzed click reaction type I

Alternatively, Cu(II) may be used, the latter one is more stable in an oxygen atmosphere, which is better for storage, and can be simply *in situ* reduced to Cu(I) by the addition of ascorbic acid. Some catalysts, such as bromo tris(triphenylphosphine)copper(I), are extremely efficient, and as low as 0.5 mol is sufficient to catalyze the reaction. Being highly lipophilic, it may be used with liquid reactants under neat conditions and without a base. If the reaction is conducted in water, the given catalyst functions as a base, if conducted in organic solvents, the addition of e.g., triethylamine is necessary.

The Cu(I)-catalyzed azide-alkyne cycloaddition (CuAAC) became a synonym for CCh (**Figure 16**).

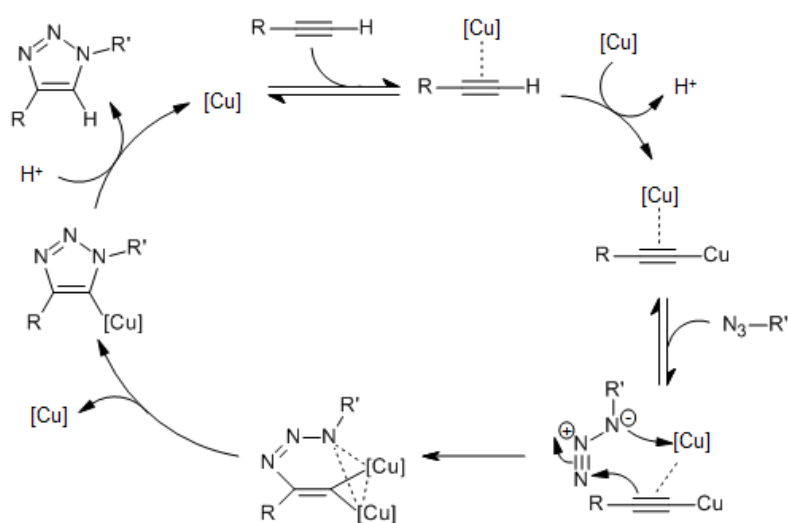


Figure 16: A mechanism scheme of Cu(I)-catalyzed azide-alkyne cycloadditions, taken over from B. T. Worell, J. A. Malik, V. V. Fokin, [42]

The CuAAC proceeds incomparably faster at room temperature compared to uncatalyzed at 100 °C. The CuAAC thus became a favorite and preferred procedure for triazoles synthesis. Triazoles are interesting pharmacophores for the variety of possible not only biomedical applications. The reactions of triazoles in living organisms are limited by Cu(I)-related toxicity, which can be overcome by alkynes (**Figure 17**) that react selectively with azides without the need of Cu(I) catalyst even *in vivo* [41,43].

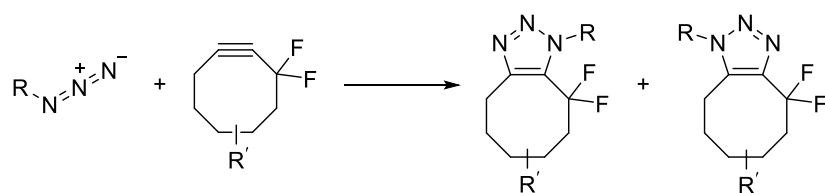


Figure 17: Example of Copper-free click chemistry

3.5.3 The use of Click chemistry

CCh enables fast production of many molecules of diverse architecture. CuAAC introduces a triazole moiety into the resulting product, which is not associated with any toxicity and is present in already approved drugs, such as rufinamide (**Figure 18**). This 1,4-disubstituted triazole structure is isosteric to peptide bond, however stable to the proteolytic action of proteases. In medicinal chemistry, CuAAC is used e.g., for production of libraries for researching the chemical space of the target, especially if the structure of the active site and its surroundings is unknown [44]. Recently the CuAAC has

been widely utilized for the synthesis of proteolysis-targeting chimeras (PROTACs) (**Figure 19**). In the latter case two active domains connected by a linker are tethered together, generally in the last reaction steps and CuAAC reaction provides the necessary yields, selectivity, and mild conditions. Beyond the medicinal chemistry, CuAAC is widely utilized in chemical biology where biological compounds (from small molecules to proteins) can be labelled *via* CuAAC with e.g., fluorophores, radioactive traces, etc. CuAAC has found particular usefulness even in material sciences where, for example surfaces of different materials (glass surface, nanoparticles...) can be easily modified by CuAAC [45].

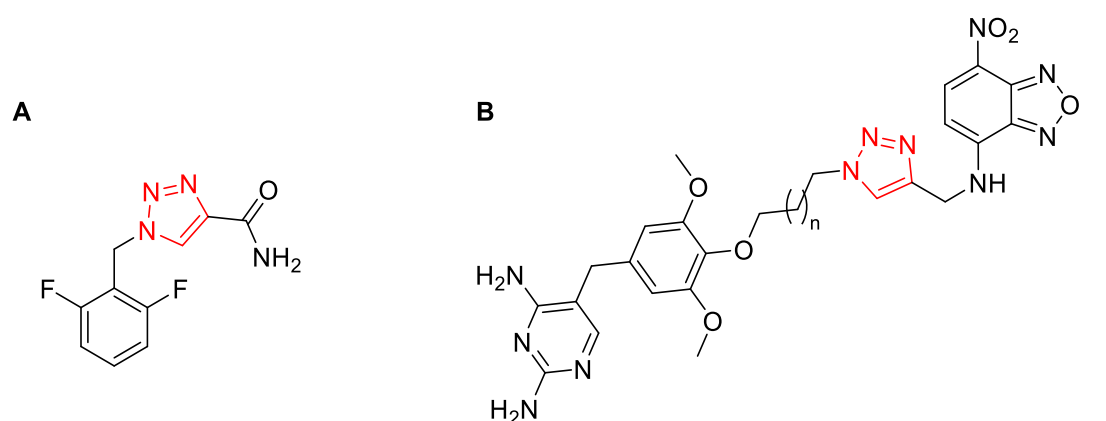


Figure 18: Examples of CuAAC utilization (triazoles are highlighted in red): A - drug rufinamide, B - fluorescently labelled trimethoprim, taken over from Phetsang, W. et al [46]

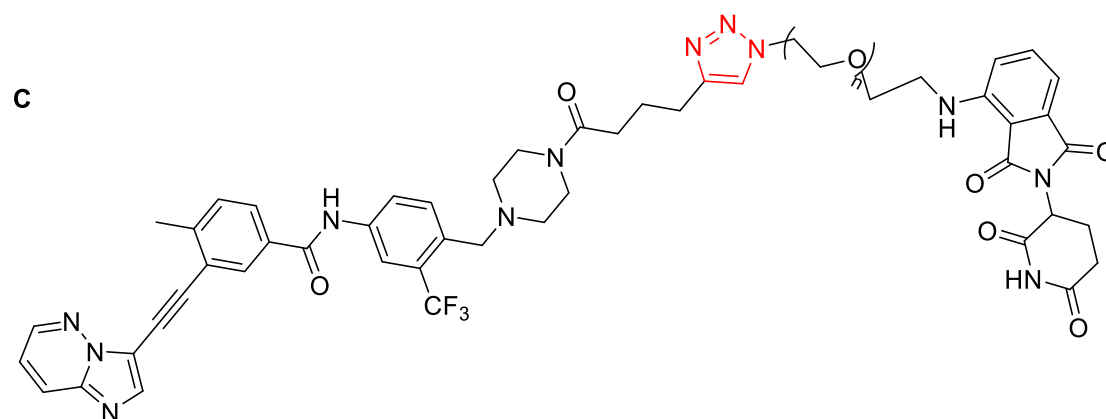


Figure 19: C - PROTAC Toolbox for Degrading BCR-ABL, taken over from Yang, YQ. et al [47]

4 Experimental part

4.1 Materials, instruments, analytical methods

All presented compounds were synthesized in the laboratories of the Department of pharmaceutical chemistry, Faculty of Pharmacy, University of Ljubljana.

Chemicals used during experiments were obtained from companies: Apollo Scientific (Bredbury, United Kingdom), Acros Organics (Geel, Belgium), Fluka (Buchs, Switzerland) and Sigma-Aldrich (Schnelldorf, Germany). Solvents were provided by: Merck (Darmstadt, Germany) and, Carlo Erba reagents (Val-de-Reuil, France). All solvents and chemicals used were not additionally purified.

Thin layer chromatography (TLC) was applied for monitoring reaction progress and column chromatography fractions. Pre-coated silica 60 F254 aluminum sheets for detection were purchased from Merck (Darmstadt, Germany). The sheets were visualized under ultraviolet (UV) light at wavelength of 254 nm and/or 366 nm. Several mobile phases were used, but mostly mixtures of hexane/ethyl-acetate or DCM/MeOH, the exact ratios are provided at the description of synthesis and purification for each compound.

Column chromatography was used for separation of different fractions of certain products. Silica gel 60 with the particle size of 0.040–0.063 mm was used as stationary phase. Exact mobile phase composition is described in detail at the description of synthesis and purification for each compound.

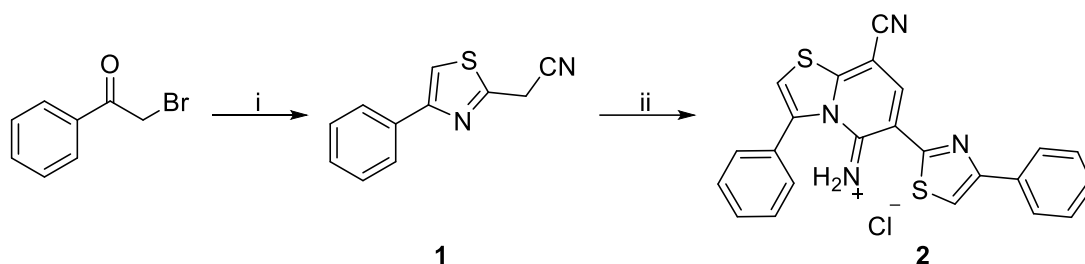
The emission spectra were recorded with a PerkinElmer LS 55 spectrofluorometer. The samples were diluted and dissolved in EtOH and imaged with a pulsed xenon lamp as excitation light source.

NMR spectra were recorded at BRUKER AVANCE III 400 MHz spectrometer. Chemical shifts are given in ppm relative to standard tetramethylsilane via solvent signal (1.50 ppm for ^1H and 39.7 ppm for ^{13}C in DMSO, and 7.26 ppm for ^1H and 77.0 for ^{13}C in CDCl_3). Melting points were obtained using Cambridge Instruments microscope equipped with heating table Reichert-Jung and thermometer Testoterm GmbH and Co. The melting points are uncorrected.

All structures, chemical formulas, and calculations of molecular weights as well Log *P* parameter were produced in Software ChemDraw professional 20.0 (PerkinElmer, Massachusetts, USA).

4.2 Synthesis of nitrogen bridgehead fused cyanopyridines

4.2.1 Synthesis of compound 1 and 2



Reagents and conditions in the synthesis of compound 2: (i) 2-cyanothioacetamide, Et₂N, THF, RT; (ii) 4 M HCl in dioxane, DMF, RT.

2-(4-Phenylthiazol-2-yl)acetonitrile (1). 2-Cyanothioacetamide (1.06 g, 10.55 mmol, 1.05 equiv) was dissolved in mixture of THF (30 mL) and Et₂N (1.7 mL), and the resulted solution was cooled in an ice bath. Bromoacetophenone (2.0 g, 10.05 mmol, 1 equiv) dissolved in THF (20 mL) was added dropwise and the reaction mixture was stirred at room temperature for 12 hours. Solvents were removed under reduced pressure, the residue was dissolved in EtOAc (60 mL) and washed with 1 M HCl (2 × 20 mL), saturated solution of NaHCO₃ (20 mL), and brine (20 mL). The organic phase was dried with anhydrous Na₂SO₄, the solvent was removed under reduced pressure to give the desired product (96%, 1.9 g) as a dark brown solid. The crude product was used in the next step without any further purification.

8-Cyano-3-phenyl-6-(4-phenylthiazol-2-yl)-5H-thiazolo[3,2-a]pyridin-5-iminium chloride (2). HCl (10 mL, 4 M in dioxane) was added to the solution of compound 1 (1.90 g, 9.5 mmol, 1 equiv) in DMF (20 mL) and the reaction mixture was stirred at 70 °C for 12 hours. After cooling the reaction mixture to RM, orange precipitate started to form, which was filtered off and dried to yield pure product 2. Solvents of the filtrate were removed under reduced pressure and the crude product was purified by flash chromatography (DCM:Hex, 1:1 to 3:1). After flash chromatography, pure fractions were joined together, solvents were removed under reduced pressure to give the desired product as an orange solid. In total, reaction yielded 158mg of final product, which is 4% of expected yield.

Chemical Formula: C₂₃H₁₅N₄S₂Cl

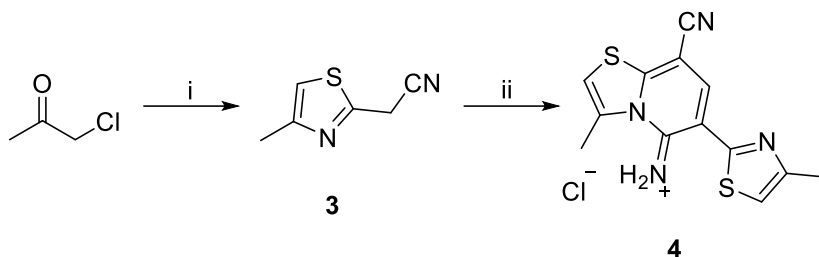
Molecular Weight: 410.51

Log P: 6.25

Melting point: 224.9–225.9 °C

¹H NMR: (400 MHz, DMSO-*d*₆): δ 8.75–7.36 (m, 13H).

4.2.2 Synthesis of compound 3 and 4



Reagents and conditions in the synthesis of compound 4: (i) 2-cyanothioacetamide, DMF, RT; (ii) 4 M HCl in dioxane, DMF, RT.

8-cyano-3-methyl-6-(4-methylthiazol-2-yl)-5H-thiazolo[3,2-*a*]pyridin-5-iminium chloride (4). 2-Cyanothioacetamide (2 g, 20 mmol, 1 equiv) was dissolved in DMF (10 mL) and the resulted solution was cooled in an ice bath. Chloroacetone (1.6 mL, 20 mmol, 1 equiv) was added dropwise and the reaction mixture was stirred at room temperature for 3 days. TLC analysis of the reaction mixture confirmed the intermediate product **3**. HCl (5 mL 4 M in dioxane) was added, and the reaction mixture was stirred at room temperature for additional 72 hours. Solvents were removed under reduced pressure and the product was purified with flash chromatography (DCM:MeOH, 50:1 to 15:1), to give the desired product as a dark yellow to orange solid.

Chemical formula: C₁₃H₁₁N₄S₂Cl

Molecular weight: 322.83

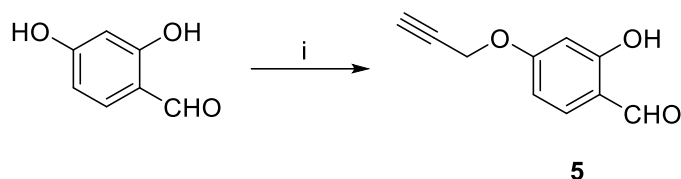
Melting point: 104–107 °C

¹H NMR: (400 MHz, Pyr-*d*₅) δ 7.77 (s, 1H), 7.03 (q, *J* = 0.9 Hz, 1H), 6.87 (q, *J* = 1.1 Hz, 1H), 2.91 (d, *J* = 1.3 Hz, 3H), 2.39 (d, *J* = 1.0 Hz, 3H).

¹³C NMR: (101 MHz, Pyr-*d*₅) δ 165.61, 160.32, 155.13, 153.26, 142.98, 132.99, 118.24, 113.60, 113.26, 108.86, 78.79, 20.56, 17.48.

4.3 Synthesis of merocyanine-type fluorescent probes for labelling lipid droplets

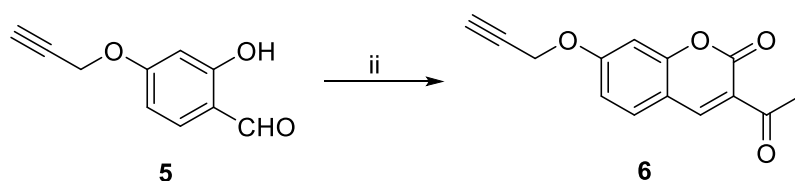
4.3.1 Synthesis of compound 5, 6, 7, 8 and 9



Reagents and conditions in the synthesis of compound 5: (i) propargyl bromide, K₂CO₃, ACN, 60 °C

2-Hydroxy-4-(prop-2-yn-1-yloxy)benzaldehyde (5). K₂CO₃ (4.03 g, 29.1 mmol, 1.03 mmol) and 2,4-dihydroxybenzaldehyde (3.91 g, 28.9 mmol, 1 equiv) were suspended in ACN (60 mL). Propargyl bromide (3.14 mL, 29.1 mmol, 1.03 equiv) was added dropwise at room temperature. After 2 hours of stirring, the reaction was heated to 60 °C in an oil bath and stirred for 12 hours. The solvents were removed under reduced pressure, the residue was suspended in ethyl acetate (60 mL) and transferred to a separatory funnel. The organic phase was washed with 1 M HCl (2 × 30 mL), saturated solution of NaHCO₃ (30 mL), and brine (30 mL). The organic phase was dried with anhydrous Na₂SO₄, and the solvent was removed under reduced pressure to give the desired product (92%, 4.58 g) as a brown solid. The crude product was used in the following step without any further purification.

Chemical formula of compound **5**: C₁₀H₈O₃



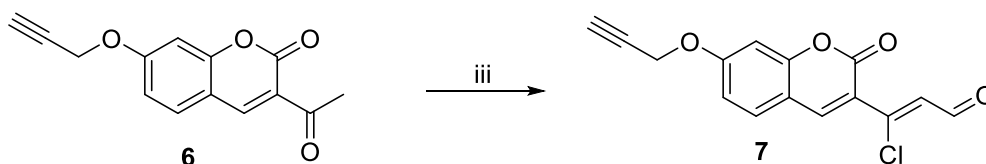
Reagents and conditions in synthesis of compound 6: (ii) ethyl acetoacetate, morpholine, ethanol, 95 °C

3-Acetyl-7-(prop-2-yn-1-yloxy)-2H-chromen-2-one (6). Crude aldehyde **5** (4.0 g, 22.7 mmol, 1 equiv), ethyl acetoacetate (4.88 mL, 45.4 mmol, 2 equiv) and morpholine (980 μL, 11.3 mmol, 0.5 equiv) were dissolved in ethanol (35 mL). The reaction mixture was refluxed (95 °C) for 12 hours. When the reaction mixture was cooled down to room temperature, the product started to precipitate and was filtered off, washed with 50% ethanol (10 mL), and dried at 60 °C in drying cabinet until a constant mass was achieved, to yield the desired product (90%, 6.5 g) as a pale brown solid.

Chemical formula of compound **6**: C₁₄H₁₀O₄

¹H NMR: (400 MHz, CDCl₃) δ 8.50 (s, 1H), 7.62–7.54 (m, 1H), 7.02–6.92 (m, 2H), 4.81 (d, *J* = 2.4 Hz, 2H), 2.71 (s, 3H), 2.61 (t, *J* = 2.4 Hz, 1H)

¹³C NMR: (101 MHz, CDCl₃) δ 195.58, 163.00, 159.71, 157.56, 147.75, 131.67, 121.35, 114.35, 112.75, 101.70, 77.36, 77.02, 56.54, 30.73.



Reagents and conditions in the synthesis of compound 7: (iii) POCl₃, DMF, 60 °C

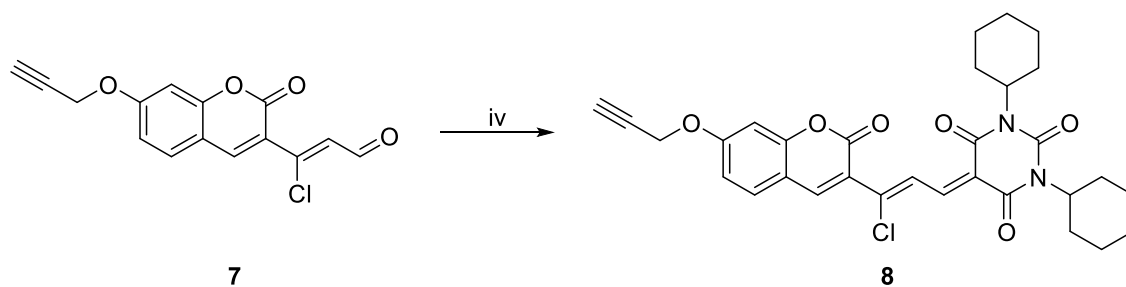
(Z)-3-Chloro-3-[2-oxo-7-(prop-2-yn-1-yloxy)-2H-chromen-3-yl]acrylaldehyde (7). POCl₃ (12.7 mL, 20.6 mmol, 4 equiv) was added dropwise to the DMF (30 mL), cooled in an ice bath and the mixture was stirred at 0 °C for 30 min. Then compound **6** (5 g, 20.6 mmol, 1 equiv) was added and the mixture was stirred for 12 hours at 60 °C. The reaction mixture was cooled down and added dropwise to the mixture of EtOAc (100 mL) and solution of Na₂CO₃ (35 g) in water (300 mL) cooled in an ice bath. After the addition, the pH of the mixture was checked and adjusted to 9. The mixture was then transferred to the separatory funnel. The organic phase was washed with water (5 × 40 mL), brine (30 mL), dried with anhydrous Na₂SO₄, and the solvent was removed under reduced pressure to give the desired product (58%, 4.2 g) as a yellow solid.

Chemical formula of compound **7**: C₁₅H₉ClO₄

¹H NMR: (400 MHz, DMSO *d*₆) δ 10.18 (d, *J* = 6.8 Hz, 1H), 8.83 (s, 1H), 7.94 (d, *J* = 8.8 Hz, 1H), 7.43 (d, *J* = 6.8 Hz, 1H), 7.15 (d, *J* = 2.4 Hz, 1H), 7.10 (dd, *J* = 8.8, 2.4 Hz, 1H), 5.00 (d, *J* = 2.4 Hz, 2H), 3.71 (t, *J* = 2.4 Hz, 1H).

¹³C NMR: (101 MHz, DMSO *d*₆) δ 192.08, 162.44, 157.29, 155.25, 145.89, 144.19, 131.70, 127.19, 117.58, 114.06, 112.70, 101.19, 79.25, 78.23, 56.47.

HRMS (ESI): *m/z* calcd for C₁₅H₉ClO₄ [M+H]⁺ 289.0262; found 289.0260.



Reagents and conditions in the synthesis of compound 8: (iv) 1,3-dicyclohexylbarbituric acid, Et_3N , RT

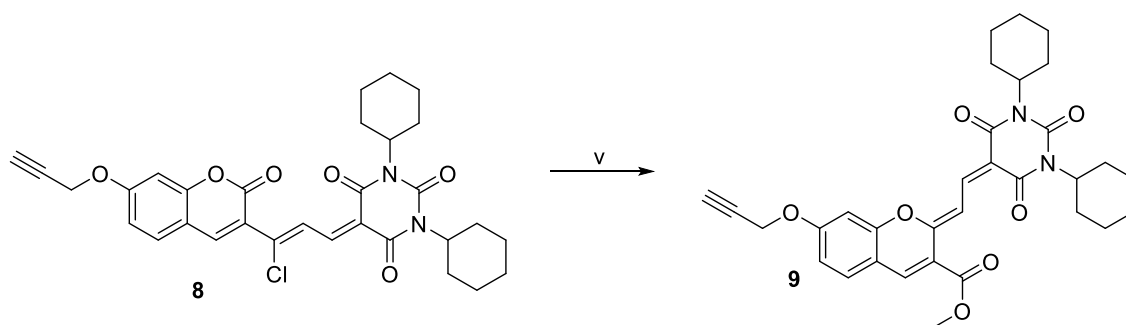
(Z)-5-{3-chloro-3-[2-oxo-7-(prop-2-yn-1-yloxy)-2H-chromen-3-yl]allylidene}-1,3-dicyclohexyl-1H,3H,5H-pyrimidine-2,4,6-trione (8). Chloropropenal 7 (500 mg, 1.37 mmol, 1 equiv) and *N,N*-dicyclohexyl barbituric acid (500 mg, 1.37 mmol, 1 equiv) were dissolved in DCM (5 mL) and the reaction mixture was stirred at room temperature overnight. Solvents were removed under reduced pressure and the product was purified with flash chromatography (Hex:EtOAc, 1:3), to give the desired product (13%, 360 mg) as an orange solid.

Chemical formula of compound 8: $C_{31}H_{31}ClN_2O_6$

1H NMR: (400 MHz, $CDCl_3$) δ 9.51 (d, $J = 11.6$ Hz, 1H), 8.62 (d, $J = 11.6$ Hz, 1H), 8.42 (s, 1H), 7.59–7.54 (m, 1H), 7.01–6.96 (m, 2H), 4.81 (d, $J = 2.4$ Hz, 2H), 4.82–4.65 (m, 2H), 2.62 (t, $J = 2.4$ Hz, 1H), 2.41–2.26 (m, 4H), 1.90–1.79 (m, 4H), 1.75–1.58 (m, 8H), 1.45–1.30 (m, 4H).

^{13}C NMR: (101 MHz, $CDCl_3$) δ 162.60, 162.19, 161.37, 157.68, 155.61, 150.66, 149.49, 144.81, 143.50, 130.69, 126.86, 119.88, 119.04, 114.47, 113.17, 101.51, 77.11, 77.07, 56.56, 55.64, 54.89, 29.32, 29.29, 26.55, 26.52, 25.41, 25.37.

HRMS (ESI): m/z calcd for $C_{31}H_{31}O_6N_2Cl$ $[M+H]^+$ 563.19430; found 563.19434.



Reagents and conditions in the synthesis of compound 9: (v) MeOH, K_2CO_3 , RT

Methyl-2-(1,3-dicyclohexyl-2,4,6-trioxohexahydropyrimidin-5-ylidene)ethylidene]-7-(prop-2-yn-1-yloxy)-2H-chromene-3-carboxylate (9). Compound **8** (61 mg, 0.11 mmol, 1 equiv) and K_2CO_3 (45 mg, 0.32 mmol, 3 equiv) were suspended in MeOH (20 mL). The reaction mixture was stirred for 12 hours at room temperature. The solvent was removed under reduced pressure and the crude product was purified with flash chromatography (Hex:EtOAc, 1:3), to give the desired product (66%, 40 mg) as a dark red solid.

Chemical formula of compound **9**: $C_{31}H_{34}N_2O_7$

Molecular weight: 558.631

Log *P*: 3.58

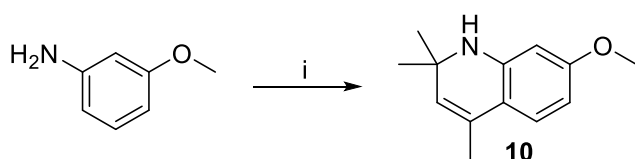
Melting point: 226.5–228.9 °C

1H NMR: (400 MHz, $CDCl_3$) δ 8.81 (d, $J = 13.2$ Hz, 1H), 8.45 (d, $J = 13.2$ Hz, 1H), 7.97 (s, 1H), 7.32 (d, $J = 8.6$ Hz, 1H), 6.88 (d, $J = 2.2$ Hz, 1H), 6.84 (dd, $J = 8.6, 2.2$ Hz, 1H), 4.79 (d, $J = 2.4$ Hz, 2H), 4.91–4.70 (m, 2H), 3.94 (s, 3H), 2.64 (t, $J = 2.4$ Hz, 1H), 2.47–2.29 (m, 4H), 1.90–1.77 (m, 4H), 1.74–1.60 (m, 4H), 1.45–1.18 (m, 8H).

^{13}C NMR: (101 MHz, $CDCl_3$) δ 163.55, 163.44, 162.97, 162.38, 159.89, 155.73, 151.12, 148.73, 140.87, 130.51, 118.99, 114.27, 113.74, 110.87, 104.78, 101.11, 77.10, 77.06, 56.46, 54.91, 53.72, 52.86, 29.38, 29.32, 26.61, 26.53, 25.45, 25.42.

HRMS (ESI): m/z calcd for $C_{31}H_{34}O_7N_2$ $[M+H]^+$ 559.2439; found 559.2438.

4.3.2 Synthesis of compound 10, 11, 12, 13, 14, 15, 16 and 17

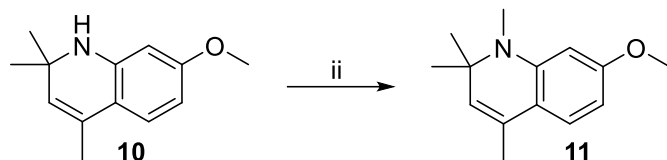


Reagents and conditions in the synthesis of compound 10: (i) acetone, $InCl_3$, 60 °C

7-Methoxy-2,2,4-trimethyl-1,2-dihydroquinoline (10). *m*-Anisidine (10 g, 81.2 mmol, 1 equiv) was dissolved in 60 ml of acetone followed by the addition of $InCl_3$. A round bottom flask with the reaction mixture was fitted with a reflux condenser and the reaction mixture was mixed at 60 °C for 2 days. The solvent was removed under reduced pressure, the residue was dissolved in a mixture of Hex:EtOAc (2:1) and filtered through a silica pad. Solvents of the filtrate were removed under reduced pressure to yield the product

(88%, 14.5 g) as a light brown oil that was used in the next step without any further purification.

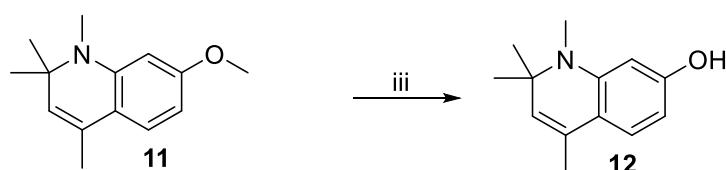
Chemical formula of compound **10**: C₁₃H₁₇NO



Reagents and conditions in synthesis of compound 11: (ii) MeI, K₂CO₃, ACN, 110 °C

7-Methoxy-1,2,2,4-tetramethyl-1,2-dihydroquinoline (11). Compound **10** (16.51 g, 81.22 mmol, 1 equiv), K₂CO₃ (22.45 g, 162.43 mmol, 2 equiv) and MeI (7.60 mL, 1.5 equiv) were added to DMF (75 mL). The reaction mixture was gradually heated up to 110 °C over 2 h and stirred at the same temperature for 12 hours. The solvents were removed under reduced pressure, and the residue was suspended in EtOAc (200 mL) and transferred to a separatory funnel. The organic layer was washed with water (5 × 50 mL), brine (50 mL), and dried with anhydrous Na₂SO₄. The solvents were removed under reduced pressure, the residue was dissolved in a mixture of Hex:EtOAc (2:1) and filtered through a silica pad. Solvents of the filtrate were removed under reduced pressure to yield the product (75%, 13 g) as light brown oil that was used in the next step without any further purification.

Chemical formula of compound **11**: C₁₄H₁₉NO

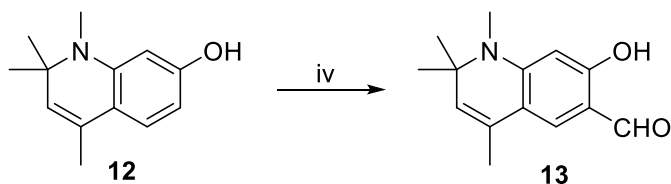


Reagents and conditions in synthesis of compound 12: (iii) BBr₃, DCM, -80 °C

1,2,2,4-Tetramethyl-1,2-dihydroquinolin-7-ol (12). Compound **11** (15 g, 69.03 mmol, 1 equiv) was dissolved in DCM and the solution was cooled to -80 °C. BBr₃ (13.1 mL, 138.05 mmol, 2 equiv) was added dropwise, and the reaction mixture was stirred for 12 hours at room temperature. The reaction mixture was cooled in an ice bath and the MeOH (110 mL) was added dropwise. The reaction mixture was transferred to a separatory funnel and washed firstly with a saturated solution of NaHCO₃ (50 mL), then with 0:1 M HCl (50 mL), and later with brine (30 mL). The organic phase was dried with anhydrous

Na₂SO₄ and the solvents were evaporated under reduced pressure and the crude product was purified by flash chromatography (Hex:EtOAc, 1:8 → 1:4), to give the desired product (56%, 7.9 g) as light brown oil.

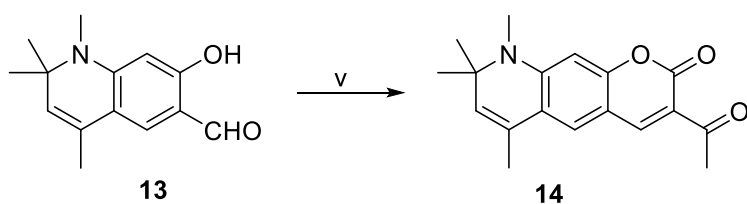
Chemical formula of compound **12**: C₁₃H₁₇NO



Reagents and conditions in synthesis of compound **13**: (iv) POCl₃, DMF (together form Vilsmeier-Haack reagent), 60 °C

7-Hydroxy-1,2,2,4-tetramethyl-1,2-dihydroquinoline-6-carbaldehyde (13). POCl₃ (12.7 mL, 20.6 mmol, 4 equiv) was added dropwise to the DMF (30 mL) and so Vilsmeier-Haack reagent was formed, then cooled in an ice bath and the mixture was stirred at 0 °C for 30 min. Then compound **12** (7.79 g, 38.32 mmol, 1 equiv) was added and the mixture was stirred for 2 h at 75 °C. The reaction mixture was cooled down and added dropwise to the mixture of EtOAc (100 mL) and solution of Na₂CO₃ (35 g) in water (300 mL) cooled in an ice bath. The pH of a mixture was adjusted to 9 by Na₂CO₃, which served as a base. The mixture was then transferred to a separatory funnel. The organic phase was washed with water (5 × 40 mL), then brine (30 mL), dried with anhydrous Na₂SO₄, and the solvent was removed under reduced pressure to give the desired product (43%, 6.6 g) as a yellow solid.

Chemical formula of compound **13**: C₁₄H₁₇NO₂



Reagents and conditions in synthesis of compound **14**: (v) methyl acetoacetate, morpholine, EtOH, 95 °C

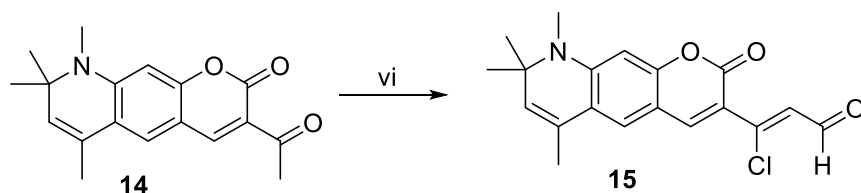
3-Acetyl-6,8,8,9-tetramethyl-8,9-dihydro-2H-pyrano[3,2-g]quinolin-2-one (14). Compound **14** was synthesized according to the procedure described for the synthesis of compound **6**. The crude product was purified by flash chromatography (Hex:EtOAc, 3:1), to give the desired product (37%, 1.5 g) as an orange solid.

Chemical formula of compound **14**: C₁₈H₁₉NO₃

¹H NMR: (400 MHz, CDCl₃) δ 8.43 (s, 1H), 7.11 (s, 1H), 6.31 (s, 1H), 5.36 (q, *J* = 1.2 Hz, 1H), 2.93 (s, 3H), 2.68 (s, 3H), 2.00 (d, *J* = 1.2 Hz, 3H), 1.42 (s, 6H).

¹³C NMR: (101 MHz, CDCl₃) δ 195.65, 160.90, 159.13, 151.25, 147.85, 130.00, 125.96, 124.03, 120.56, 115.94, 108.23, 95.65, 58.35, 31.94, 30.67, 29.15, 18.67.

HRMS (ESI): *m/z* calcd for C₁₈H₂₀O₃N₂ [M+H]⁺ 298.1438; found 298.1434.



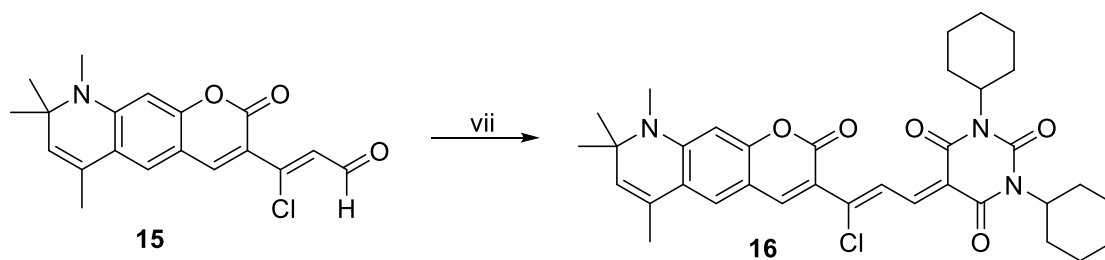
Reagents and conditions in synthesis of compound 15: (vi) POCl₃, DMF, 60 °C

(Z)-3-chloro-3-(6,8,8,9-tetramethyl-2-oxo-8,9-dihydro-2H-pyrano[3,2-g]quinolin-3-yl)acrylaldehyde (15). Compound 15 was synthesized according to the procedure described for the synthesis of compound 7. The crude product was purified with flash chromatography (Hex/EtOAc, 3/1,) to give the desired product (69%, 1.2 g) as a dark red solid.

Chemical formula of compound 15: C₁₉H₁₈ClNO₃

¹H NMR: (400 MHz, CDCl₃) δ 10.25 (d, *J* = 7.0 Hz, 1H), 8.32 (s, 1H), 7.66 (d, *J* = 7.0 Hz, 1H), 7.08 (s, 1H), 6.28 (s, 1H), 5.38 (q, *J* = 1.1 Hz, 1H), 2.93 (s, 3H), 2.01 (d, *J* = 1.1 Hz, 3H), 1.43 (s, 6H).

¹³C NMR: (101 MHz, CDCl₃) δ 192.54, 158.40, 157.18, 151.11, 145.54, 144.86, 130.31, 125.89, 123.24, 120.77, 112.59, 108.45, 95.50, 58.45, 31.99, 29.18, 18.73.



Reagents and conditions in synthesis of compound 16: (vii) 1,3 dicyclohexylbarbituric acid, Et₃N, RT

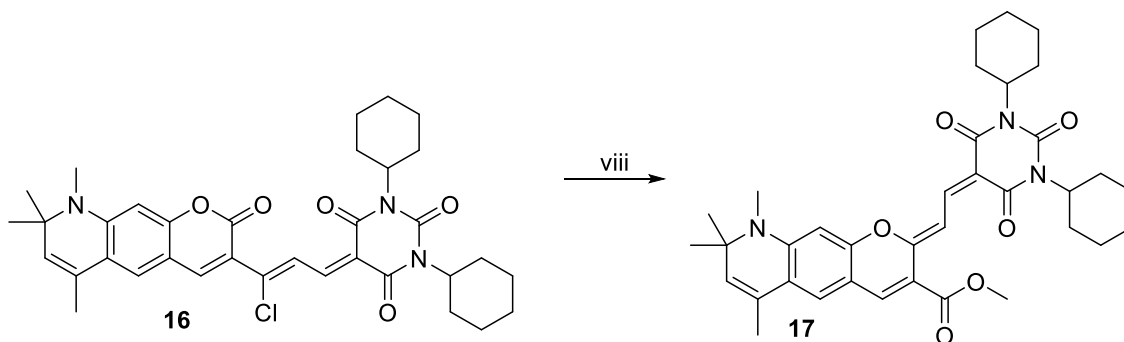
(Z)-5-[3-chloro-3-(6,8,8,9-tetramethyl-2-oxo-8,9-dihydro-2H-pyrano[3,2-g]quinolin-3-yl)allylidene]-1,3-dicyclohexyl-1H,3H,5H-pyrimidine-2,4,6-trione (16). Compound 16 was synthesized according to the procedure described

for the synthesis of compound **8**. The crude product was purified by flash chromatography (Hex:EtOAc, 5:1 → 3:1), to give the desired product (21%, 462 mg) as an orange solid.

Chemical formula of compound **16**: C₃₅H₄₀ClN₃O₅

¹H NMR: (400 MHz, CDCl₃) δ 9.55 (d, *J* = 11.9 Hz, 1H), 8.67 (d, *J* = 11.9 Hz, 1H), 8.32 (s, 1H), 7.09 (s, 1H), 6.33 (s, 1H), 5.37 (q, *J* = 1.1 Hz, 1H), 4.87–4.66 (m, 2H), 2.95 (s, 3H), 2.43–2.28 (m, 4H), 2.01 (d, *J* = 1.1 Hz, 3H), 1.90–1.77 (m, 4H), 1.71–1.60 (m, 4H), 1.43 (s, 6H), 1.40–1.16 (m, 8H).

¹³C NMR: (101 MHz, CDCl₃) δ 162.62, 161.55, 158.44, 157.19, 151.08, 150.88, 150.78, 146.23, 145.23, 130.20, 126.00, 124.20, 123.28, 120.76, 116.70, 114.54, 109.03, 95.74, 58.50, 55.36, 54.51, 32.06, 29.31, 29.17, 26.57, 26.53, 26.42, 25.43, 25.40, 18.75.



Reagents and conditions in synthesis of compound 17: (viii) MeOH, K₂CO₃, RT

Methyl-2-{2-[1,3-dicyclohexyl-2,4,6-trioxotetrahydropyrimidin-5(2*H*)-ylidene]ethylidene}-6,8,8,9-tetramethyl-8,9-dihydro-2*H*-pyrano[3,2-*g*]quinoline-3-carboxylate (17**)**. Compound **17** was synthesized according to the procedure described for the synthesis of compound **9**. The crude product was purified with flash chromatography (Hex:EtOAc, 4:1 → 2:1), to give the desired product (67%, 193 mg) as a dark blue powder.

Chemical formula of compound **17**: C₃₆H₄₃N₃O₆

Molecular weight: 613.755

Log *P*: 4.7

Melting point: 268.3–270.1 °C

¹H NMR: (400 MHz, CDCl₃) δ 8.88 (d, *J* = 13.6 Hz, 1H), 8.53 (d, *J* = 13.6 Hz, 1H), 8.03 (s, 1H), 6.94 (s, 1H), 6.36 (s, 1H), 5.35 (q, *J* = 1.1 Hz, 1H), 4.94–4.82 (m, 1H), 4.81–4.68

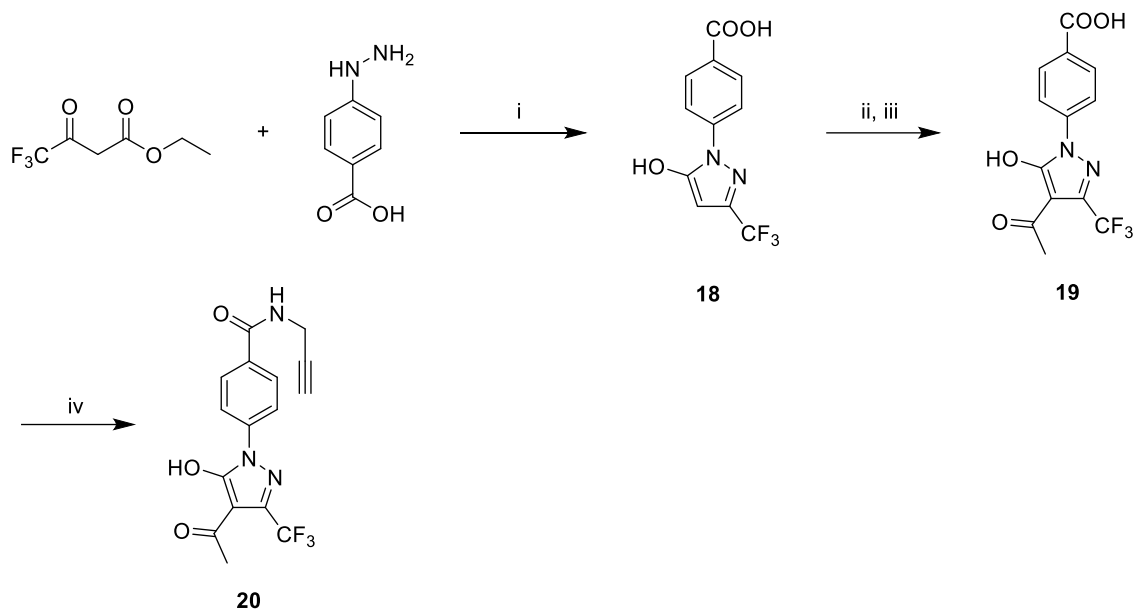
(m, 1H), 3.90 (s, 3H), 2.95 (s, 3H), 2.47–2.28 (m, 4H), 1.96 (d, $J = 1.1$ Hz, 3H), 1.87–1.75 (m, 4H), 1.73–1.58 (m, 4H), 1.41 (s, 6H), 1.39 1.16 (m, 8H).

^{13}C NMR: (101 MHz, CDCl_3) δ 163.29, 163.03, 161.95, 161.80, 156.36, 150.82, 150.56, 148.06, 141.61, 129.34, 124.92, 122.22, 120.00, 112.57, 108.94, 106.21, 102.84, 94.70, 57.64, 53.64, 52.33, 51.56, 30.69, 28.53, 28.42, 28.23, 25.74, 25.64, 24.58, 24.55, 17.70.

HRMS (ESI): m/z calcd for $\text{C}_{36}\text{H}_{43}\text{N}_3\text{O}_6$ $[\text{M}+\text{H}]^+$ 614.3225; found 614.3218.

4.4 Ligands

4.4.1 Synthesis of ligand 20



Reagents and conditions in synthesis of compound 20: (i) AcOH, 115 °C; (ii) triethyl orthoacetate, 110 °C; (iii) 6 M HCl, EtOH, 110 °C; (iv) propargylamine, EDC, DMAP, Et₃N, DCM, RT.

4-(5-Hydroxy-3-(trifluoromethyl)-1H-pyrazol-1-yl)benzoic acid (18). Ethyl 4,4,4-trifluoro-3-oxobutanoate (4.06 mL, 27.75 mmol, 1 equiv) and 4-hydrazinylbenzoic acid (4.22 g, 27.75 mmol, 1 equiv) were dissolved in AcOH (10 mL) and mixed at 140 °C overnight. The reaction was cooled down, 5 mL of water was added and the mixture was stirred for 1 h. Precipitate was filtered off and dried to give the desired product (66%, 5 g) as light gray solid.

¹H NMR (400 MHz, DMSO-*d*₆) δ 13.02 (bs, 2H), 8.11–8.05 (m, 2H), 7.95–7.89 (m, 2H), 5.98 (s, 1H).

¹³C NMR (101 MHz, DMSO-*d*₆) δ 166.78, 154.51, 141.39 (q, *J* = 37.5 Hz), 141.32, 130.55, 129.02, 121.34, 121.30 (q, *J* = 268.8 Hz), 86.10.

4-(4-Acetyl-5-hydroxy-3-(trifluoromethyl)-1H-pyrazol-1-yl)benzoic acid (19). Compound 18 (2.90 g, 10.65 mmol, 1 equiv) and triethyl orthoacetate (2.34 mL, 12.79 mmol, 1.2 equiv) were stirred at 120 °C for 20 min. 96% v/v EtOH (5 mL) and 6 M HCl (0.5 mL) were added and the reaction mixture was mixed at 120 °C for 3 hours. Then the reaction mixture was cooled down, and the precipitate was filtered off and dried to give the desired product (55%, 4.8 g) as a light gray solid.

¹H NMR (400 MHz, DMSO-*d*₆) δ 10.49 (bs, 2H), 8.12–8.06 (m, 2H), 8.04–7.98 (m, 2H), 2.42 (s, 3H).

¹³C NMR (101 MHz, DMSO-*d*₆) δ 188.21, 166.90, 161.09, 141.69, 139.19 (q, *J* = 37.4 Hz), 130.49, 128.02, 120.90 (q, *J* = 269.3 Hz), 120.24, 102.54, 26.18.

HRMS (ESI): *m/z* calcd for C₁₃H₉N₂O₄F₃ [M-H]⁻ 313.0442; found 313.0441.

4-(4-Acetyl-5-hydroxy-3-(trifluoromethyl)-1*H*-pyrazol-1-yl)-*N*-(prop-2-yn-1-yl)benzamide (20). Carboxylic acid **19** (1.0 g, 3.18 mmol, 1 equivalent), propargylamine (263 mg, 4.77 mmol, 1.5 equiv), triethylamine (1.76 mL, 12.7 mmol, 4 equiv) and DMAP (389 mg, 4.77 mmol, 1 equiv) were dissolved in DCM (50 mL) and cooled in an ice bath. EDC (911 mg, 4.77 mmol, 1.5 equiv) was added and the reaction mixture was stirred at room temperature for 12 hours. The reaction mixture was transferred to a separatory funnel and washed firstly with 1 M HCl (4 × 40 mL), then with brine (30 mL), and dried over anhydrous Na₂SO₄. Solvents were removed under reduced pressure and the crude product was crystallized from MeOH to give the desired compound (45%, 0.6 g) as a light orange solid.

Chemical formula: C₁₆H₁₂F₃N₃O₃

Molecular weight: 351.2582

Log *P*: 1.85

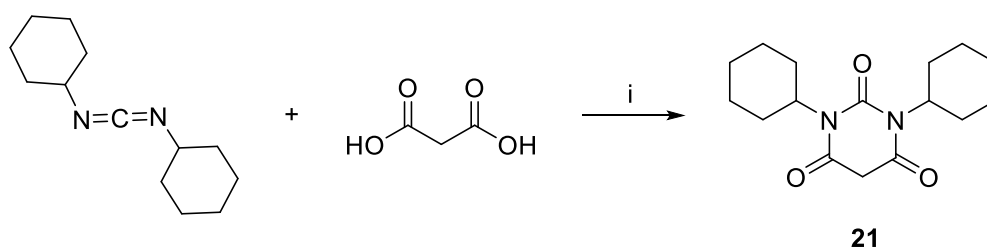
Melting point: 197.7–200.7 °C

¹H NMR (400 MHz, DMSO-*d*₆) δ 9.23 (bs, 2H), 8.98 (t, *J* = 5.5 Hz, 1H), 8.0–7.90 (m, 4H), 4.07 (dd, *J* = 5.5, 2.5 Hz, 2H), 3.13 (t, *J* = 2.5 Hz, 1H), 2.45 (s, 3H).

¹³C NMR (101 MHz, DMSO-*d*₆) δ 188.22, 165.30, 161.03, 140.70, 139.02 (q, *J* = 37.2 Hz), 130.84, 128.26, 120.97 (q, *J* = 269.3 Hz), 120.10, 102.38, 81.37, 72.92, 28.56, 26.68.

HRMS (ESI): *m/z* calcd for C₁₆H₁₂N₃O₃F₃ [M-H]⁻ 350.0758; found 350.0758.

4.4.2 Synthesis of ligand 21



Reagents and conditions in synthesis of compound 21: (i) THF, 0 °C.

Malonic acid (2.52 g, 24.23 mmol, 1 equiv) was dissolved in THF (25 mL) and cooled down in an ice bath. Dicyclohexylcarbodiimide (DCC) (10 g, 48.47 mmol, 2 equiv) was dissolved in THF (25 mL) and added dropwise to the solution of malonic acid in THF. A precipitate of dicyclohexylurea derivative started to form and the reaction mixture was stirred at room temperature for 12 hours. The precipitate was filtered off and the THF of the filtrate was removed under reduced pressure to yield the desired product (70%, 6.3 g) as a white solid.

Name: 1,3-dicyclohexyl-1,3-diazinane-2,4,6-trione

Chemical formula: C₁₆H₂₄N₂O₃

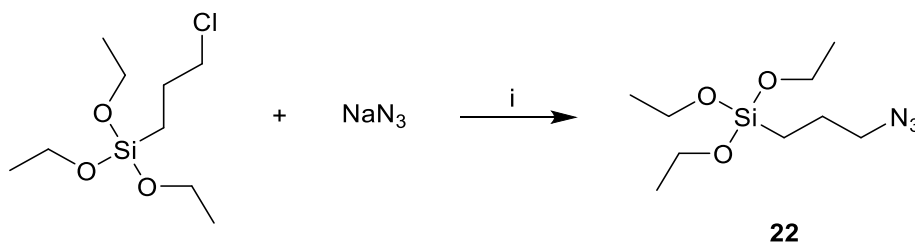
Molecular weight: 292.38

Log *P*: 2.21

Melting point: 178.2–180.3 °C

¹H NMR (400 MHz, CDCl₃) δ 4.59 (tt, *J* = 12.2, 3.7 Hz, 2H), 3.60 (s, 2H), 2.33–2.18 (m, 4H), 1.89–1.78 (m, 4H), 1.70–1.56 (m, 6H), 1.42–1.11 (m, 6H).

4.4.3 Synthesis of compound 22



Reagents and conditions in synthesis of compound 22: (i) ACN, 75 °C.

3-(Chloropropyl)triethoxysilane (3 mL, 12.46 mmol, 1 equiv) and NaN₃ (2.02 g, 31.15 mmol, 2.5 equiv) were added to ACN (30 mL) This reaction ran as mentioned by Zhang

[48]. The reaction mixture was stirred overnight at 75 °C. The following day ACN was removed under reduced pressure and the residue was suspended in 20 ml of diethyl ether. Solid part was filtered off and diethyl ether was removed under reduced pressure to yield the desired product (91%) as a colorless liquid. The product was stored under argon at -20 °C.

Name: (3-azidopropyl)triethoxysilane

Chemical formula: C₉H₂₁N₃O₃Si

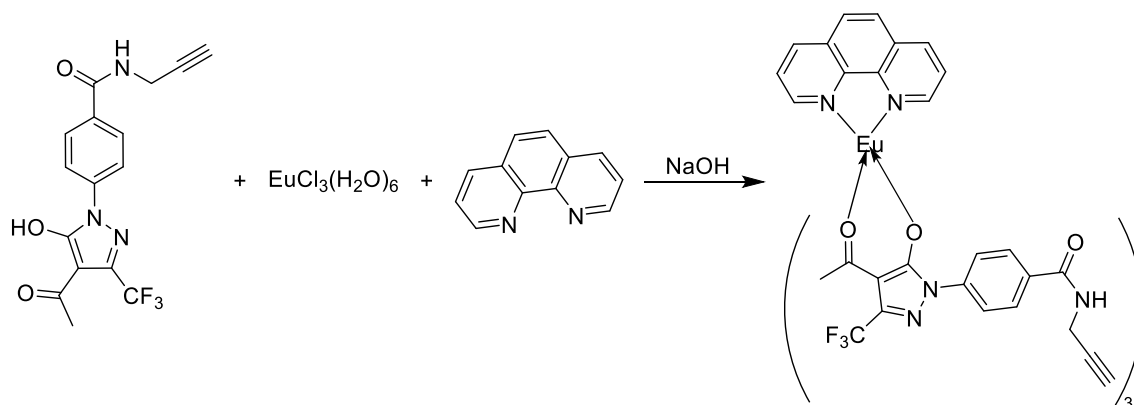
Molecular weight: 247.37

Real mass: 2.8 g (91%)

¹H NMR (400 MHz, CDCl₃) δ 3.83 (q, *J* = 7.0 Hz, 6H), 3.27 (t, *J* = 7.0 Hz, 2H), 1.77–1.65 (m, 2H), 1.23 (t, *J* = 7.0 Hz, 9H), 0.73–0.63 (m, 2H).

4.5 Click reactions with lanthanide complexes

4.5.1 Synthesis of lanthanide complexes



Example of a reaction for synthesis of lanthanide complexes

4.5.1.1 General procedure for the synthesis of complexes

Main ligand (3 mmol) and auxiliary ligand – phenanthroline/bipyridine (1 mmol) were dissolved in anhydrous ethanol (5 mL). 1 M NaOH (3 mL, 3 mmol) was added dropwise to the solution and the reaction mixture was heated to 60 °C. Lanthanide salt (100 mL) was dissolved in 1.5 mL of distilled water and was added dropwise to the solution of ligands. After adding lanthanide salt, the precipitation started to form. The reaction was mixed for 12 hours at 60 °C. Then the reaction mixture was cooled down, precipitate filtered, washed with 50% EtOH and dried at RT. Prepared complexes were examined under UV light at 365 nm. Complexes with europium emitted red, terbium ones bright

yellow, and dysprosium ones orange light. Synthesized complexes are summarized in **Tables 1–3**.

Table 1: Summary of complexes synthesized with terbium

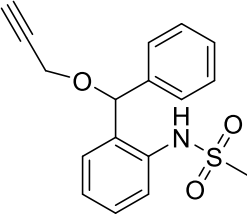
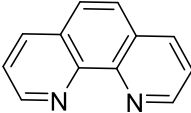
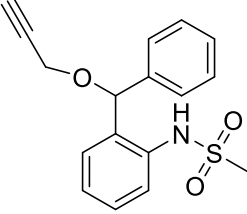
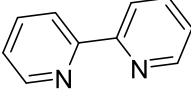
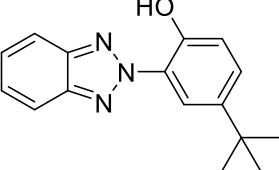
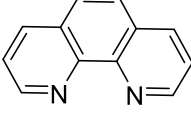
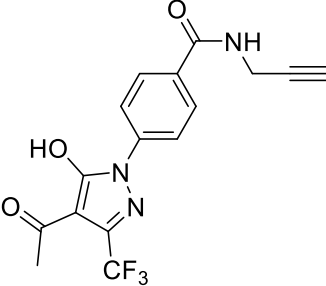
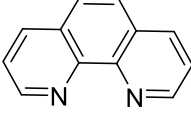
Name	Lanthanide	Main ligand	Auxiliary ligand
SPJB1C	$\text{TbCl}_3(\text{H}_2\text{O})_6$		
SPJB2C	$\text{TbCl}_3(\text{H}_2\text{O})_6$		
SPJB7C	$\text{Tb}(\text{NO})_3(\text{H}_2\text{O})_5$		
SPJB11C	$\text{Tb}(\text{NO})_3(\text{H}_2\text{O})_5$		

Table 2: Summary of complexes synthesized with dysprosium

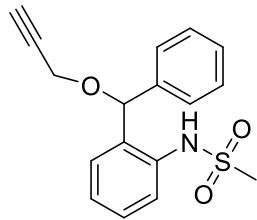
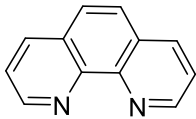
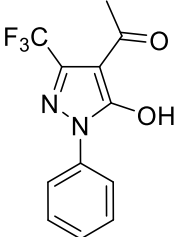
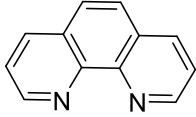
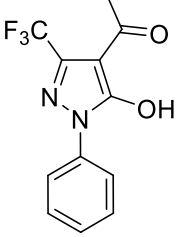
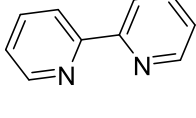
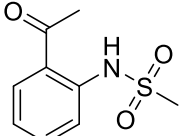
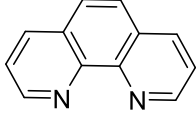
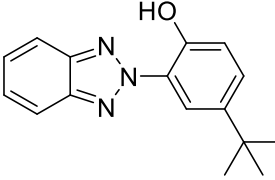
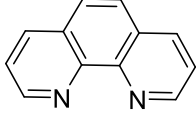
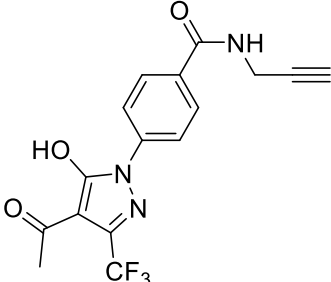
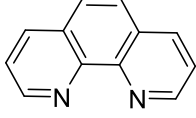
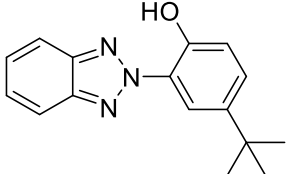
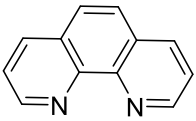
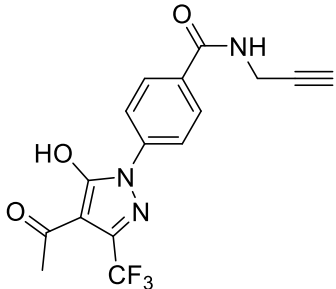
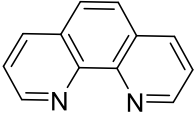
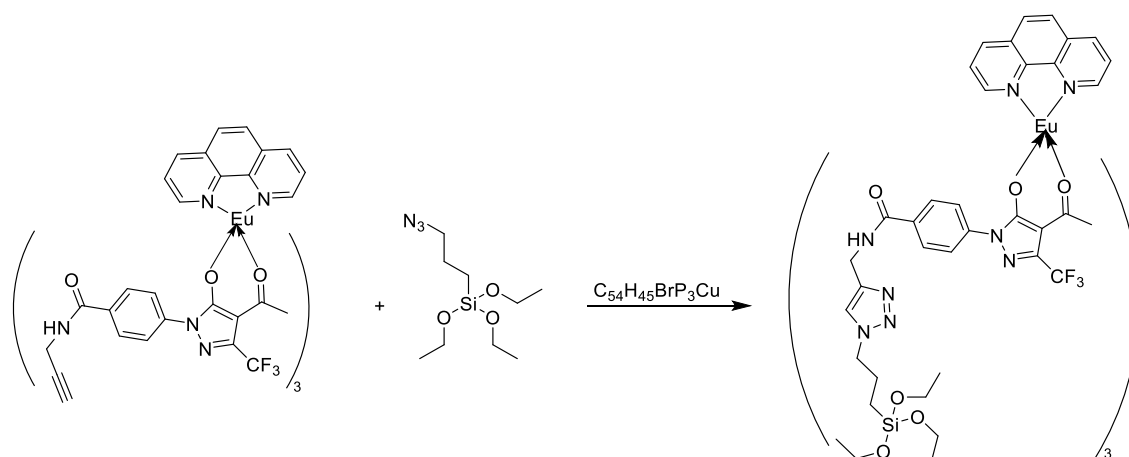
Name	Lanthanide	Main ligand	Auxiliary ligand
SPJB3C	DyCl ₃ (H ₂ O) ₆		
SPJB4C	DyCl ₃ (H ₂ O) ₆		
SPJB5C	DyCl ₃ (H ₂ O) ₆		
SPJB6C	DyCl ₃ (H ₂ O) ₆		
SPJB8C	DyCl ₃ (H ₂ O) ₆		
SPJB12C	DyCl ₃ (H ₂ O) ₆		

Table 3: Summary of complexes synthesized with europium

Name	Lanthanide	Main ligand	Auxiliary ligand
SPJB9C	EuCl ₃ (H ₂ O) ₆		
SPJB10C	EuCl ₃ (H ₂ O) ₆		

4.5.2 Click chemistry with lanthanide complex



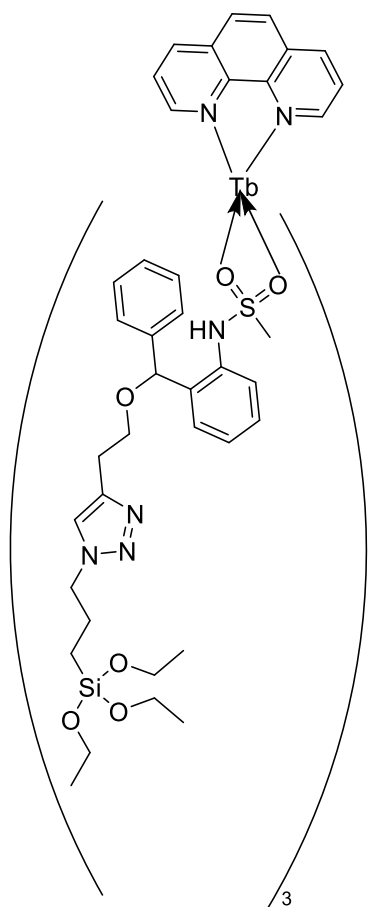
Example of a click reaction with europium complex, in this case LC-10CC was synthesized

4.5.2.1 General procedure for click reaction

. Lanthanide complex (1 mmol) and azide **22** (1.5 mmol) were dissolved in DCM (1 mL). Catalyst tris(triphenylphosphine)copper(I) bromide (0.05 mmol) was added to the solution, and the reaction was stirred at 40 °C for 12 hours. Then the product will be attached to glass. This will be done in collaboration with a research group at the Institute “Jožef Stefan” in Ljubljana, Slovenia.

4.5.2.2 Compound LC-2CC

A name could not be generated for this structure.



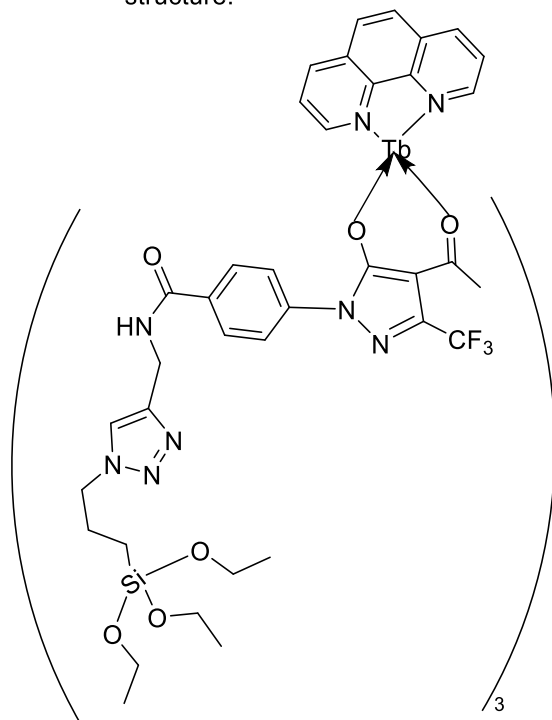
Chemical formula: $C_{87}H_{104}EuF_9N_{20}O_{18}Si_3$

Molecular weight: 2125.12

Expected yield: 76.83 mg

4.5.2.3 Compound LC-11CC

A name could not be generated for this structure.



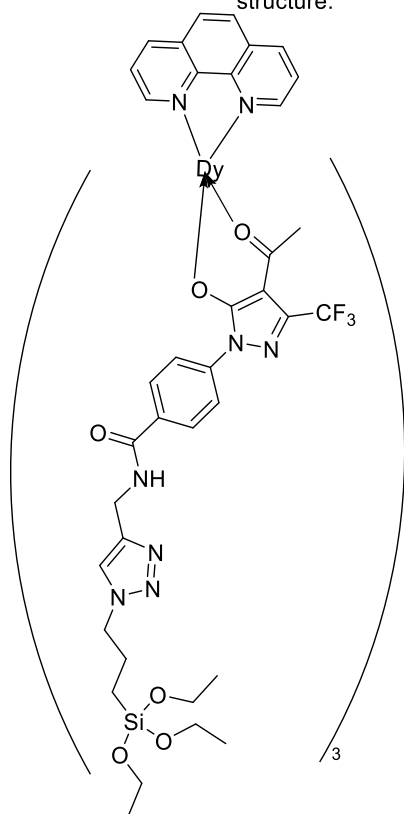
Chemical formula: $C_{87}H_{104}F_9N_{20}O_{18}Si_3Tb$

Molecular weight: 2132.08

Expected yield: 76.70 mg

4.5.2.4 Compound LC-12CC

A name could not be generated for this structure.



Chemical formula: $C_{87}H_{104}DyF_9N_{20}O_{18}Si_3$

Molecular weight: 2135.65

Expected yield: 76.63 mg

5 Results and discussion

Nitrogen bridgehead fused cyanopyridines, merocyanine-type fluorescent probes, and new ligands with corresponding lanthanide complexes were synthesized. All cited procedures were modified by my consultant in laboratory. Most steps of reactions were checked on TLC, final products and some intermediate products were purified by column chromatography, when possible. ^1H and ^{13}C NMR spectra were recorded for the most of the synthesized compounds. Melting points were measured for final compounds.

Two cyanopyridines were re-synthesized (compound **2** and **4**) according to Pajk and Živec [49] with suitable modification based on the laboratory experience. This type of compounds was discovered by a student as side product during the synthesis of 2-(4-methylthiazol-2-yl)acetonitrile (**Figure 1**) [1].

It was later established that the side product can be synthesized also from 2-(4-methylthiazol-2-yl)acetonitrile dissolved in DMF and by addition of strong anhydrous acid (e.g. HCl in dioxane). Besides methylthiazole derivative, we synthesized also phenylthiazole derivative. These types of compounds are fluorophores and emit in the green region. They are also sensitive to pH and could be potentially used as pH probes. We measured pH-dependent emission of compound **4** and PNV-7 (**Figure 20, 21 and 22**) (the compound was synthesized by another student) [50].

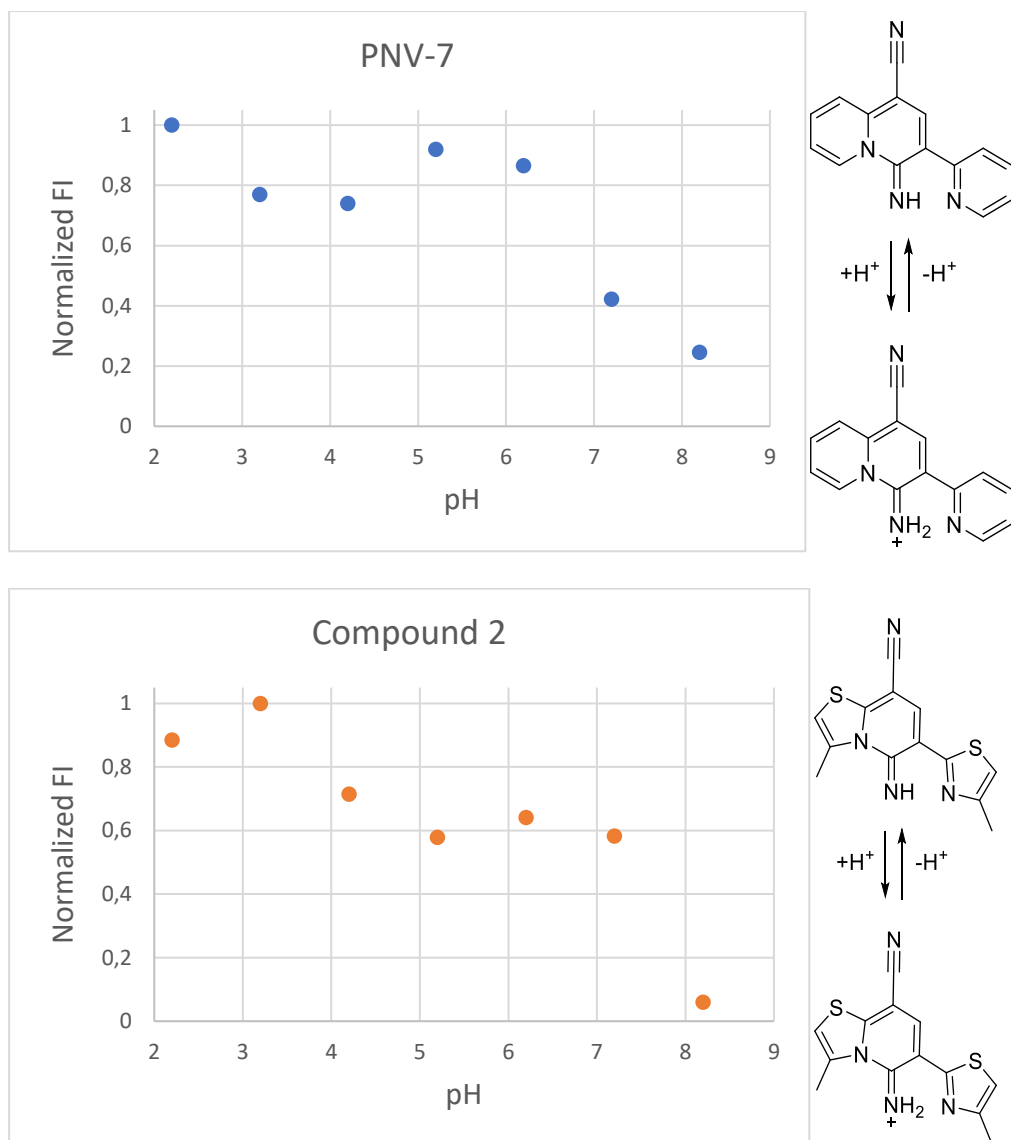


Figure 20: Emission intensity at 530 nm for PNV-7 and 525 nm for compound 2 at different pH values. On the right side, there are structures and proposed protonated/non-protonated species

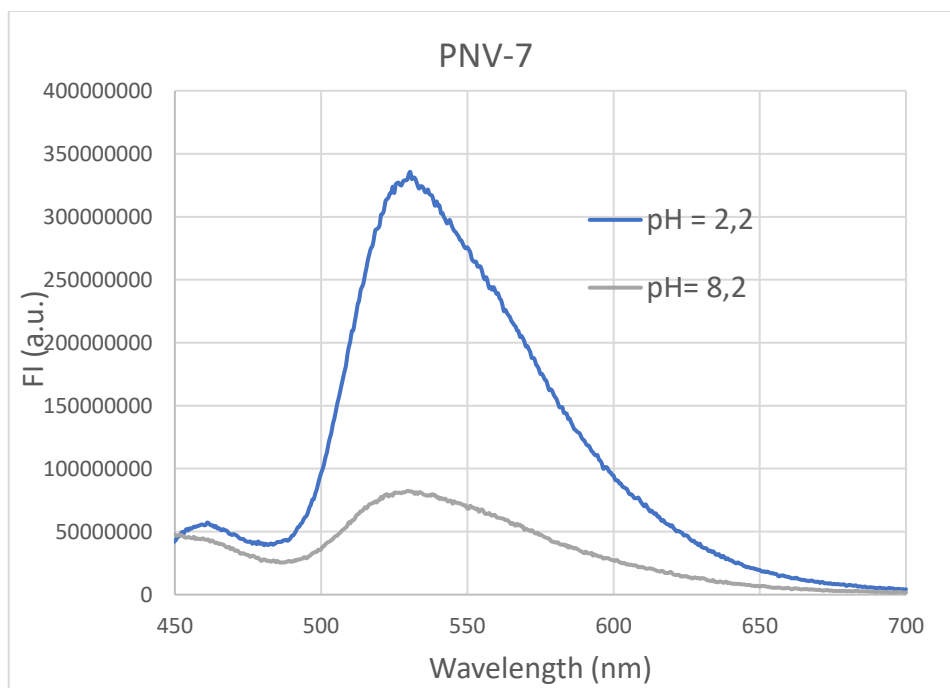


Figure 21: Emission spectrum of PNV-7 at pH 2.2 and 8.2

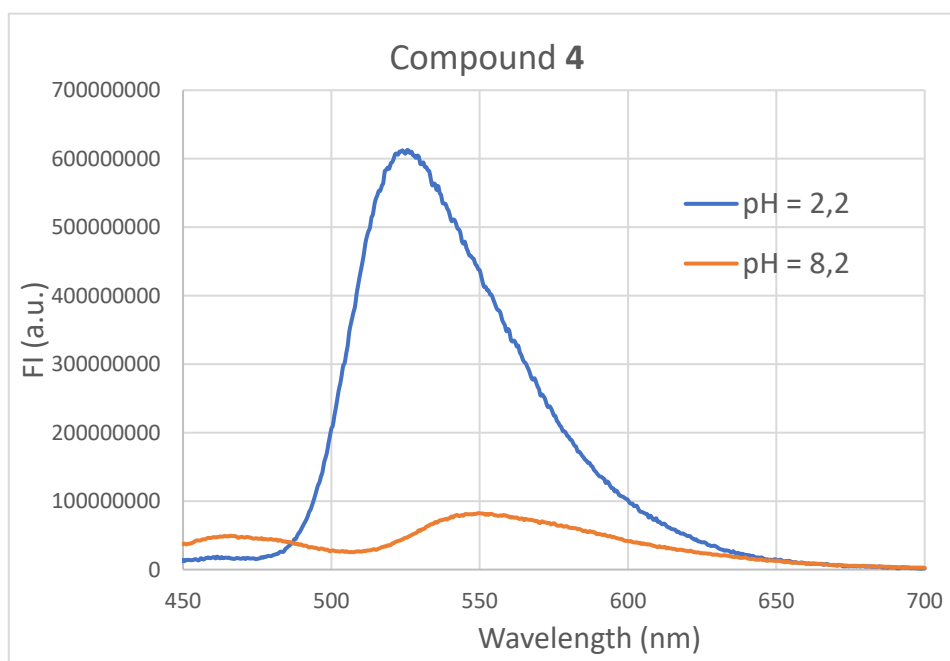


Figure 22: Emission spectrum of compound 4 at pH 2.2 and 8.2

Both compounds exhibited higher emission intensity at lower pH and poor emission at neutral pH (pH = 8). These pH values were chosen to demonstrate the difference in emission between low and neutral pH of compound 4 and PNV-7. Emission spectra indicated that emission first increases at around pH = 6 and then there was an even higher increase at pH = 1–3. This could be the consequence of the protonation of thiazole or pyridine. Nevertheless, these preliminary results were encouraging, however,

additional measurements will be made by other students with more pH points to exactly establish the relationship between the emission and pH. Additionally, the influence of incubation will be tested. We performed measurements immediately after the solutions were prepared in buffer mentioned below, however, it might take longer to establish the equilibrium. All conditions and whole procedure was set by my consultant in the lab. Compound 2 was poorly soluble in sodium phosphate/citrate buffer, therefore we did not do similar pH dependence with it. Emission spectra of compound 4 and PNV-7 are presented above (**Figure 21** and **22**).

Regarding the reaction mechanism, we presume that DMF forms some reactive species with added 4 M HCl in dioxane that in turn reacts with 2-(4-methylthiazol-2-yl)acetonitrile. The product then reacts with another 2-(4-methylthiazol-2-yl)acetonitrile to yield the final product, the proposed mechanism is given in **Figure 23**. The yields were low; however, the reaction is simple, and the final product can be further purified by crystallization. We performed column chromatography and the product started to precipitate (compound 2) in two test tubes.

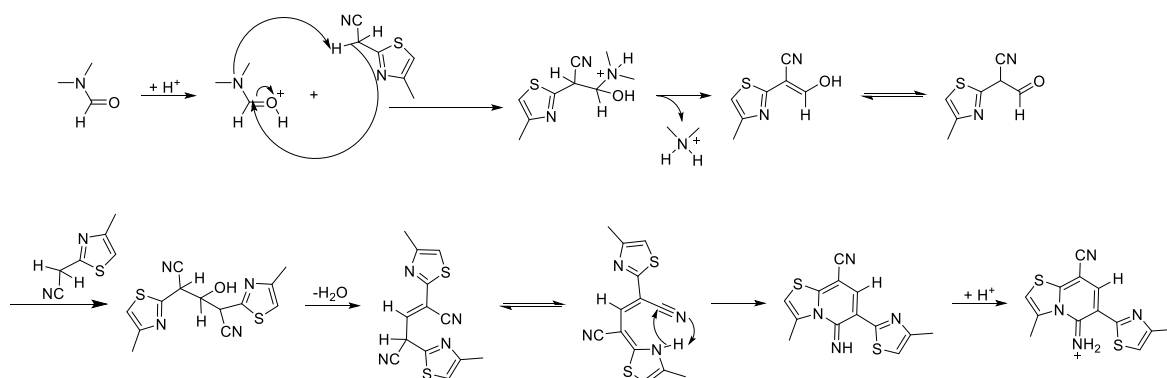


Figure 23: Proposed mechanism for the synthesis of bridgehead fused cyanopyridines.

In the next part of this thesis, two derivatives of merocyanine dye were synthesized. We intended to investigate the influence of the electron-donating group on the emission (**Figure 2**). Instead of diethylamino group we planned to introduce an ether, the weaker electron-donating capability should blue-shift the emission spectrum. The second compound has an electron donating group incorporated into a more rigid 1,2,2,4-tetramethyl-1,2-dihydroquinoline, which should produce a red-shift in the emission spectrum.

Except for the first starting stages, the end stages were the same for both compounds. As for compound **9**, the synthesis started with Williamson ether synthesis, where the propargyl group was introduced [51]. This step is based on nucleophilic substitution type 2. The latter is useful for further derivatization since it enables click chemistry. Formation of substituted chromene followed by Knoevenagel condensation where morpholine acted as a base catalyst to yield compound **6** [52]. In the next step, the Vilsmeier-Haack reagent, prepared in situ from POCl₃ and DMF, was combined with chromene **6**, and the reaction turned dark red [53]. All three procedures were modified according to instruction of my consultant. The imine intermediate was then hydrolyzed to form 3-chromyl-3-chloropropenal (**Figure 24**).

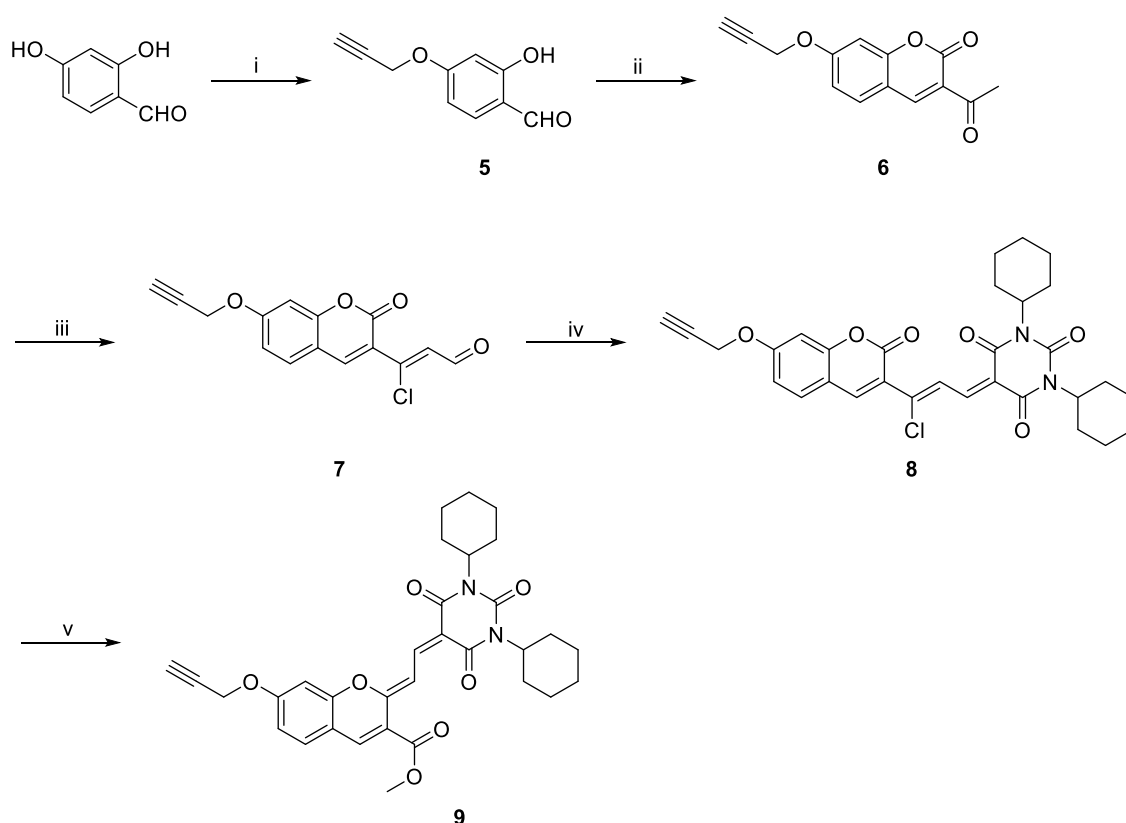


Figure 24: Reagents and conditions in synthesis of compound **9**: (i) propargyl bromide, K₂CO₃, ACN, 60 °C; (ii) ethyl acetoacetate, morpholine, ethanol, 95 °C; (iii) POCl₃, DMF, 60 °C; (iv) 1,3-dicyclohexylbarbituric acid, Et₃N, RT; (v) MeOH, K₂CO₃, RT.

In the next step, (*Z*)-3-chromyl-3-chloropropenal reacted with a derivative of barbituric acid (ligand **21**), but the latter reacted with the starting material to 2nd level, so the undesirable side product was formed. The reaction was repeated and the ratio between starting materials was adjusted in favor of (*Z*)-3-chromyl-3-chloropropenal. This modification was not sufficient, and the reaction was conducted with several solvents: DMF, acetone, and DCM, the last one turned out to be the best one. In the last step, the

final product was formed after adding methanol and K_2CO_3 into product from previous reaction. *Z*-configurations were confirmed by X-ray diffraction [2].

The second synthesized merocyanine dye is compound **17** (**Figure 25**). First three steps followed procedures described by Belov [54]. In the first step, *m*-anisidine reacted with acetone and $InCl_3$ worked as a catalyst to form 7-methoxy-2,2,4-trimethyl-1,2-dihydroquinoline (**10**). The secondary amine of the latter was methylated with MeI to form compound **11**. This was followed by the cleavage of methyl ether with BBr_3 . This step was technically the most demanding since we had to add BBr_3 at $-80\text{ }^\circ\text{C}$ and quenching of the reaction mixture with MeOH was dangerous because of the formation of HBr. In the next step, a formyl moiety was introduced with the Vilsmeier-Haack reagent, formed in situ from DMF and $POCl_3$, to afford the aldehyde **13** [55]. Other steps were analogous to the synthesis of compound **7**. *Z*-conformations were verified by X-ray diffraction [2].

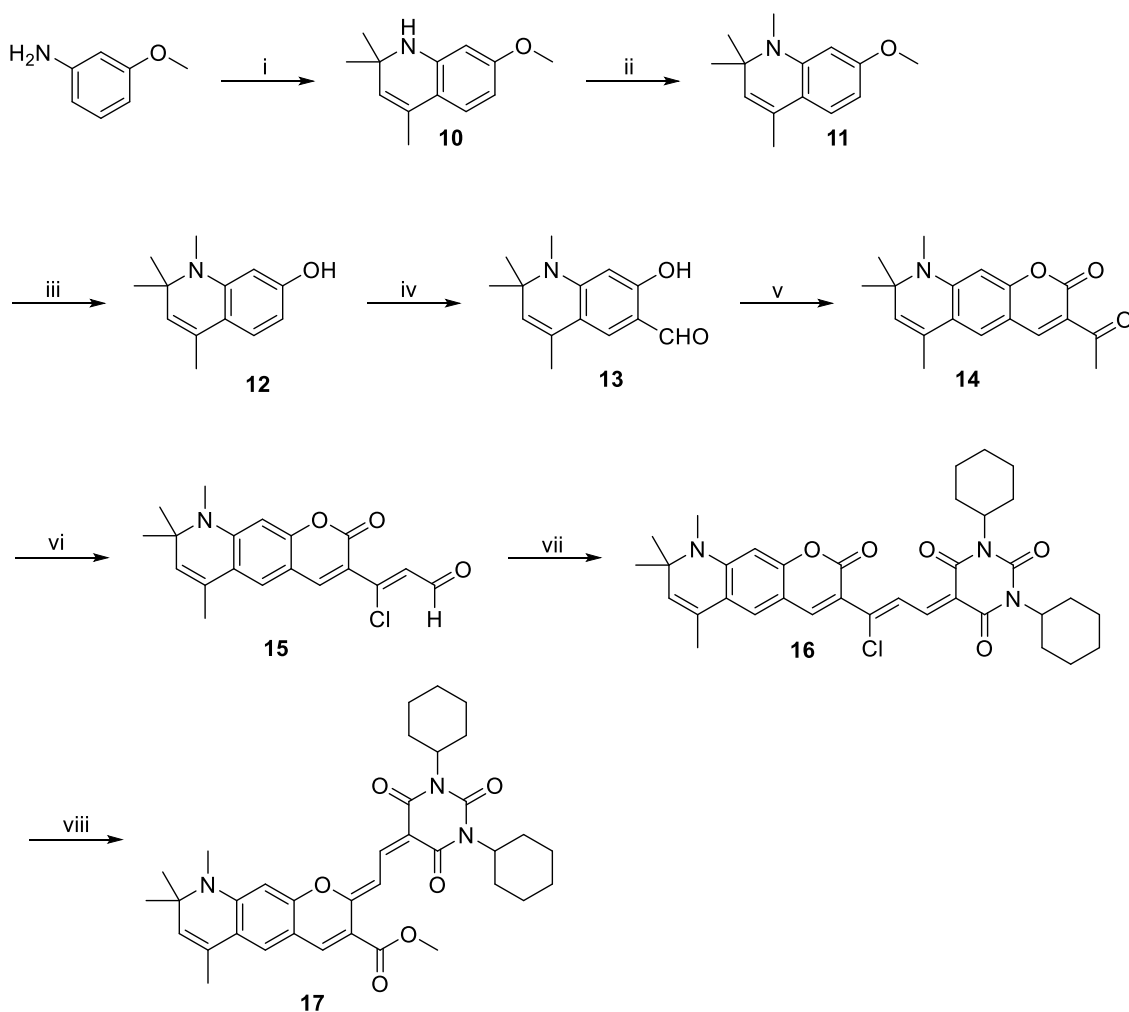


Figure 25: Reagents and conditions in the synthesis of compound 17: (i) acetone, InCl₃, 60 °C; (ii) MeI, K₂CO₃, ACN, 110 °C; (iii) BBr₃, DCM, -80 °C; (iv) POCl₃, DMF (produce in situ Vilsmeier-Haack reagent), 60 °C; (v) methyl acetoacetate, morpholine, EtOH, 95 °C; (vi) POCl₃, DMF, 60 °C; (vii) 1,3-dicyclohexylbarbituric acid, Et₃N, RT; (viii) MeOH, K₂CO₃, RT

Emission properties of the produced compounds **9** and **17** were then evaluated. Interestingly, the emission of compound **9** was very weak, on the contrary compound **17** exhibited strong emission in red region, and as expected the absorption and emission spectra were red-shifted compared to the emission spectra of **PPB-12**, which served as comparison for emission measurements (**Figure 26**). More rigid 1,2,2,4-tetramethyl-1,2-dihydroquinoline of compound **17** should provide better quantum yield and molar extinction coefficient, however, we did not have time to measure these two intrinsic variables, but they will be measured in future. According to preliminary experiments, probe **17** slowly labels lipid droplets and is in this application inferior to **PPB-12**. Slow labeling may be due to increased lipophilicity because of the introduction of 1,2,2,4-tetramethyl-1,2-dihydroquinoline. Lipid droplet probe must be soluble in water

to some extent to be able to migrate from cell culture medium to lipid droplets inside the cell and too high lipophilicity prevents this process.

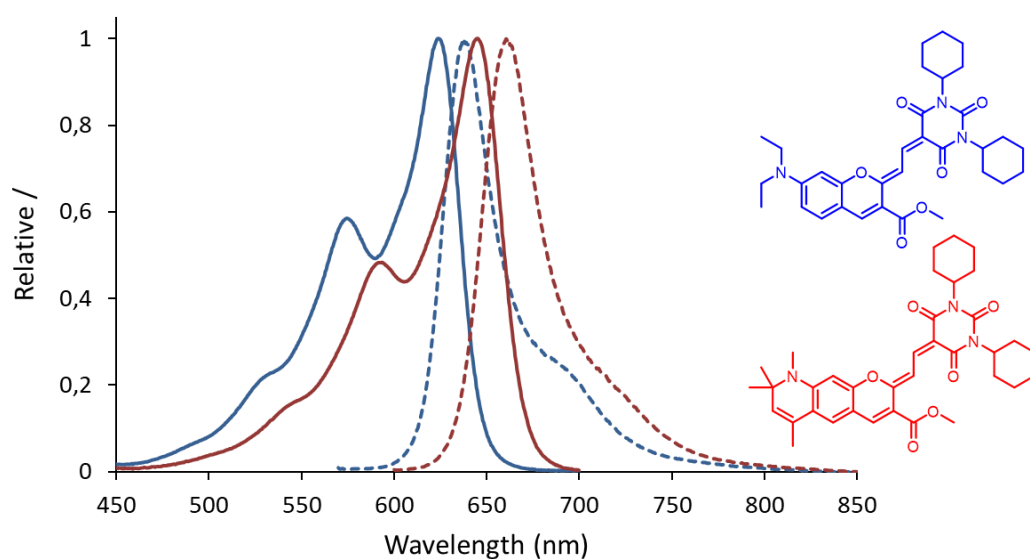


Figure 26: Comparison of absorption (solid line) and emission (dashed line) spectra of PPB-12 (blue lines) and probe 17 (red lines) dissolved in EtOH, structures of the probes on the right are highlighted in the corresponding color.

We managed to synthesize twelve different lanthanide complexes with europium, dysprosium, or terbium. Four LCs, which emit in visible light proceeded with CCh. CCh is a simple, fast procedure, which allows high yields [56]. The best four LCs (**SPJB2C**, **SPJB10C**, **SPJB11C**, **SPJB12C**) reacted with azide **22**, resulting in the formation of triazole moiety (**LC-2CC**, **LC-10CC**, **LC-11CC**, **LC-12CC**), as described by Croissant [57].

The synthesis of ligand **20** includes three steps. In the first step, ethyl 4,4,4-trifluoro-3-oxobutanoate reacts with 4-hydrazinylbenzoic acid. It is an exothermic reaction, therefore it is held in an ice bath, however only hydrazone is formed at first, to close the ring to pyrazole, higher temperatures and overnight stirring were needed. In the second step, we added triethyl-orthoacetate to introduce acetyl group. First two steps followed procedure described by Holzer and Bieringer [58]. In the last step, as designed by Hassan [59], we dissolved the product from the previous reaction in DMF and added propargylamine triethylamine, *N,N*-dimethylpyridin-4-amine (DMAP), and 1-ethyl-3-(3-dimethylaminopropyl)carbodiimide (EDC in form of hydrochloride). In this coupling reaction, amide bond is formed between propargylamine and pyrazole derivative.

Complexes were synthesized from ligand 20 and other ligands that were bought or prepared by other students previously. Ligands showed sufficient purity and contained alkyne bond, which enables further derivatization with terminal azides necessary for CCh. The procedure was simple; ligands were dissolved in EtOH, NaOH solution was added to deprotonate them, then lanthanide salt dissolved in water was added. However, the exact amount of each reagent had to be used, so all were weighted on an analytical balance. Usually, a precipitate started to be formed immediately after the addition of lanthanide salt. The reaction mixture was stirred overnight, and the precipitate was filtered off and dried. Solid products were investigated under UV light for emission. The aim was to investigate new ligands if they produce luminescent complexes. Therefore, not all the ligands had incorporated alkyne or azide moiety, they would be incorporated in the future if the complex had good emission. The second aim was to produce complexes with silyl ether that would be incorporated on the glass surface. This will be done in collaboration with a research group at the Institute “Jožef Stefan” in Ljubljana, Slovenia.

This was already successfully achieved with europium complexes; however, the europium possesses only one strong emission band with a maximum at 615 nm, others being much less intense. For ratiometric temperature measurements ratio of the intensity of two maxima is calculated and plotted against the temperature. The maxima in question have of course different temperature coefficients. In the case of europium, usual maxima at 615 nm and 590 nm are taken, however as it can be seen in **Figure 27**, the emission intensity at 590 nm is low, increasing the error of measurement.

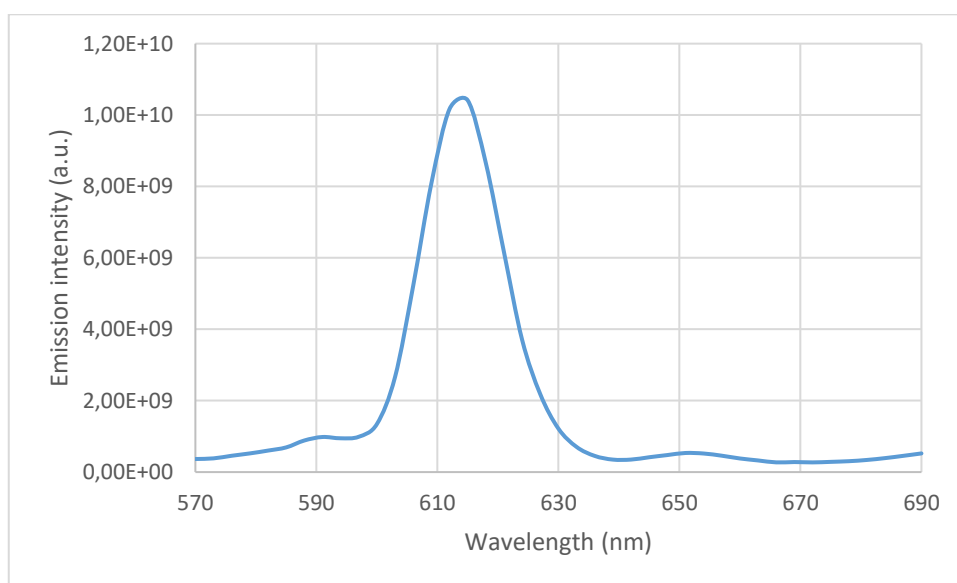


Figure 27: An example of emission of europium complex applied to the glass.

On the contrary terbium and dysprosium complexes have more emission bands with more evenly distributed emission intensity (**Figure 28**). However, the temperature coefficients are not known for these maxima; in the worst case, they are similar making the system less sensitive to temperature changes. This will be tested in the future. NMR is not possible to measure, because lanthanide complexes are paramagnetic. Mass spectrometry did not work, because of desintegration of LCs. In the future, crystallization of good emitting complexes will be done with following X-ray diffraction experiments.

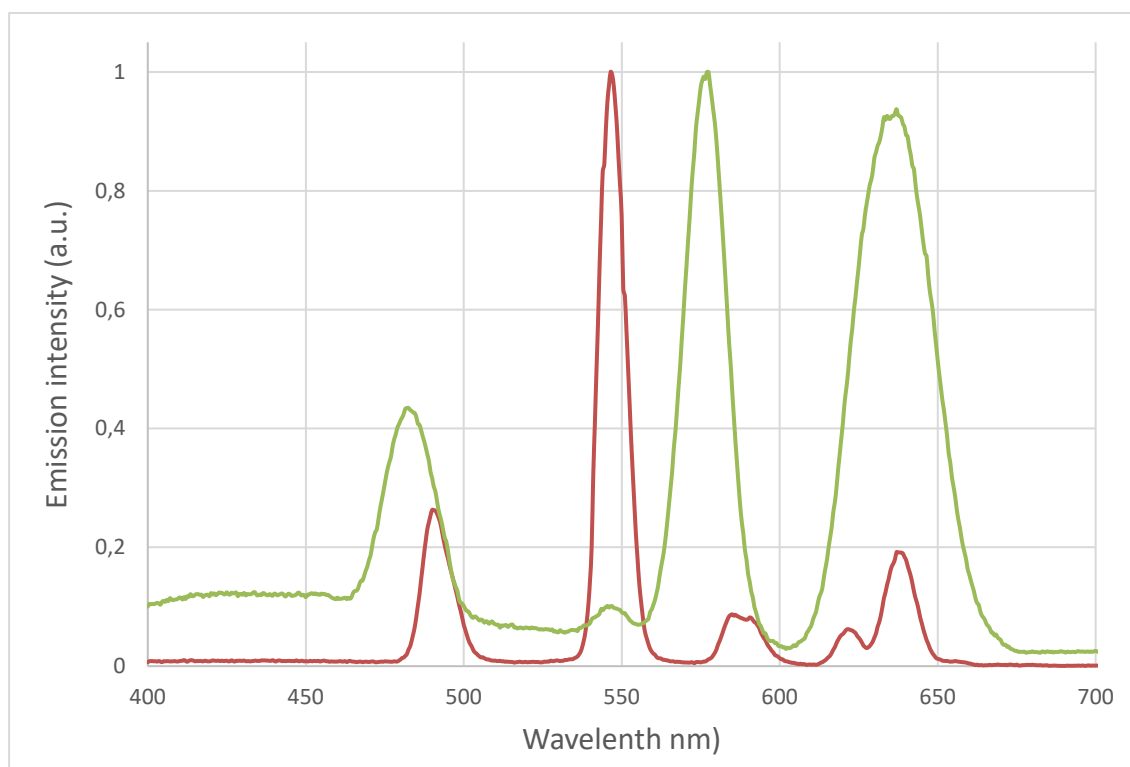


Figure 28: Normalized emission spectra of terbium (red) and dysprosium (green) complex dissolved in EtOH

6 Conclusion

During my diploma thesis, two derivatives of cyanopyridines, two derivatives of merocyanines fluorescent probes, and twelve lanthanide complexes were synthesized. It was discovered, that cyanopyridines are formed as a side product. Compound **4** showed better emission spectra at lower pH, but to make a conclusion, these measurements must be retested and conditions should be modified in the future, for instance, to include different incubation times.

In the synthesis of merocyanine dyes, electron-donating groups were incorporated into the structure of a former dye with a diethylamino group. As electron-donating groups, we chose ether (compound **9**) and 1,2,2,4-tetramethyl-1,2-dihydroquinoline (compound **17**). The emission of the latter was more promising. The red-shift in emission was confirmed as expected. The incorporated rigid structure should provide better quantum yields and molar extinction coefficient, but these two will be measured in the future. Substance **17** is less soluble in water compared to a former dye because of a more lipophilic structure, which may be the reason, why it shows a slower ability to label lipid droplets, but additional tests and structural modification must be done in the future, as well.

The last part of my diploma thesis was the synthesis of lanthanide complexes with the following CCh of chosen complexes according to their fluorescence under UV light. As lanthanide ions, Tb, Eu and Dy were chosen. We synthesized complexes with silyl ether, that will be incorporated on the glass surface at the Institute "Jožef Stefan" in Ljubljana, Slovenia. This has already been done with some of Eu complexes. Tb and Dy include more emission bands, but their emission coefficients are not known, yet. For ratiometric temperature measurements, the ratio of the intensity of two maxima is calculated and plotted against the temperature. These complexes are considered possible thermometers, but more experiments must be done in the future to determine their use in this area .

7 References

1. BEVK, A. Substitution of tetrahydropyran with cyclopentane in InhA inhibitors and optimisation of resulting enantiomers separation. *Diploma thesis* **2019**.
2. PAJK, S. Unpublished data.
3. Sanderson, M.J.; Smith, I.; Parker, I.; Bootman, M.D. Fluorescence microscopy. *Cold Spring Harb Protoc* **2014**, 2014, pdb.top071795, doi:10.1101/pdb.top071795.
4. Ishikawa-Ankerhold, H.C.; Ankerhold, R.; Drummen, G.P. Advanced fluorescence microscopy techniques--FRAP, FLIP, FLAP, FRET and FLIM. *Molecules* **2012**, 17, 4047-4132, doi:10.3390/molecules17044047.
5. Baryshnikov, G.; Minaev, B.; Ågren, H. Theory and Calculation of the Phosphorescence Phenomenon. *Chem Rev* **2017**, 117, 6500-6537, doi:10.1021/acs.chemrev.7b00060.
6. Feng, G.; Zhang, G.Q.; Ding, D. Design of superior phototheranostic agents guided by Jablonski diagrams. *Chem Soc Rev* **2020**, 49, 8179-8234, doi:10.1039/d0cs00671h.
7. Lakowicz, R.J. *Principles of Fluorescence Spectroscopy*, 3rd ed.; Springer: New York, 2006. ISBN 978-0387-31278-1
8. Jameson, D.M.; Croney, J.C.; Moens, P.D.J. Fluorescence: Basic concepts, practical aspects, and some anecdotes. *Biophotonics, Pt A* **2003**, 360, 1-43.
9. Deng, Q.S.; Zhu, Z.C.; Shu, X.W. Spectrally resolved luminescence lifetime detection for measuring the energy splitting of the long-lived excited states. *Spectrochimica Acta Part a-Molecular and Biomolecular Spectroscopy* **2020**, 224, doi:10.1016/j.saa.2019.117434.
10. Genovese, D.; Cingolani, M.; Rampazzo, E.; Prodi, L.; Zaccheroni, N. Static quenching upon adduct formation: a treatment without shortcuts and approximations. *Chemical Society Reviews* **2021**, 50, 8414-8427, doi:10.1039/d1cs00422k.
11. Yan, L.; Rueden, C.T.; White, J.G.; Eliceiri, K.W. Applications of combined spectral lifetime microscopy for biology. *Biotechniques* **2006**, 41, 249, 251, 253 passim, doi:10.2144/000112251.
12. Chen, H.Y.; Zhao, J.Z.; Lin, J.Z.; Dong, B.L.; Li, H.; Geng, B.; Yan, M. Two-photon fluorescent probes for detecting the viscosity of lipid droplets and its application in living cells. *Rsc Advances* **2021**, 11, 8250-8254, doi:10.1039/d0ra09683k.
13. Listenberger, L.L.; Brown, D.A. Fluorescent detection of lipid droplets and associated proteins. *Curr Protoc Cell Biol* **2007**, Chapter 24, Unit 24.22, doi:10.1002/0471143030.cb2402s35.
14. Mallela, S.K.; Patel, D.M.; Ducasa, G.M.; Merscher, S.; Fornoni, A.; Al-Ali, H. Detection and Quantification of Lipid Droplets in Differentiated Human Podocytes. *Methods Mol Biol* **2019**, 1996, 199-206, doi:10.1007/978-1-4939-9488-5_17.
15. Ma, Q.; Wang, J.; Li, Z.; Lv, X.; Liang, L.; Yuan, Q. Recent Progress in Time-Resolved Biosensing and Bioimaging Based on Lanthanide-Doped Nanoparticles. *Small* **2019**, 15, e1804969, doi:10.1002/smll.201804969.
16. Cho, U.; Chen, J.K. Lanthanide-Based Optical Probes of Biological Systems. *Cell Chem Biol* **2020**, 27, 921-936, doi:10.1016/j.chembiol.2020.07.009.
17. Geißler, D.; Linden, S.; Liermann, K.; Wegner, K.D.; Charbonnière, L.J.; Hildebrandt, N. Lanthanides and quantum dots as Förster resonance energy

- transfer agents for diagnostics and cellular imaging. *Inorg Chem* **2014**, *53*, 1824-1838, doi:10.1021/ic4017883.
18. Goryacheva, O.A.; Beloglazova, N.V.; Vostrikova, A.M.; Pozharov, M.V.; Sobolev, A.M.; Goryacheva, I.Y. Lanthanide-to-quantum dot Förster resonance energy transfer (FRET): Application for immunoassay. *Talanta* **2017**, *164*, 377-385, doi:10.1016/j.talanta.2016.11.054.
 19. Shuvaev, S.; Starck, M.; Parker, D. Responsive, Water-Soluble Europium(III) Luminescent Probes. *Chemistry* **2017**, *23*, 9974-9989, doi:10.1002/chem.201700567.
 20. SeethaLekshmi, S.; Ramya, A.R.; Reddy, M.L.P.; Varughese, S. Lanthanide complex-derived white-light emitting solids: A survey on design strategies. *Journal of Photochemistry and Photobiology C-Photochemistry Reviews* **2017**, *33*, 109-131, doi:10.1016/j.jphotochemrev.2017.11.001.
 21. Pantulap, U.; Arango-Ospina, M.; Boccaccini, A.R. Bioactive glasses incorporating less-common ions to improve biological and physical properties. *J Mater Sci Mater Med* **2021**, *33*, 3, doi:10.1007/s10856-021-06626-3.
 22. Zhang, R.; Yuan, J. Responsive Metal Complex Probes for Time-Gated Luminescence Biosensing and Imaging. *Acc Chem Res* **2020**, *53*, 1316-1329, doi:10.1021/acs.accounts.0c00172.
 23. Gedam, S.C.; Thakre, P.S.; Dhoble, S.J. Luminescence and spectroscopic studies of halosulfate phosphors: a review. *Luminescence* **2015**, *30*, 187-197, doi:10.1002/bio.2712.
 24. Bodman, S.E.; Butler, S.J. Advances in anion binding and sensing using luminescent lanthanide complexes. *Chem Sci* **2021**, *12*, 2716-2734, doi:10.1039/d0sc05419d.
 25. Wang Liding; Zhao; Zifeng; Wei Chen; Wei, H.; Liu Zhiwei; Bian Zuqiang; Chunhui, H. Review on the Electroluminescence Study of Lanthanide Complexes. *Advanced Optical Materials* **2019**, *7*, doi:10.1002/adom.201801256.
 26. Xu, D.; Liu, M.; Huang, Q.; Chen, J.; Huang, H.; Deng, F.; Wen, Y.; Tian, J.; Zhang, X.; Wei, Y. One-step synthesis of europium complexes containing polyamino acids through ring-opening polymerization and their potential for biological imaging applications. *Talanta* **2018**, *188*, 1-6, doi:10.1016/j.talanta.2018.05.003.
 27. Li, D.; Shao, N.; Sun, X.; Zhang, G.; Li, S.; Zhou, H.; Wu, J.; Tian, Y. Self-assembly of Terbium(III)-based metal-organic complexes with two-photon absorbing active. *Spectrochim Acta A Mol Biomol Spectrosc* **2014**, *133*, 134-140, doi:10.1016/j.saa.2014.05.038.
 28. Niu, H.Y.; Huang, D.W.; Niu, C.G. Time-gated fluorescence sensor for trace water content determination in organic solvents based on covalently immobilized europium ternary complex. *Sensors and Actuators B-Chemical* **2014**, *192*, 812-817, doi:10.1016/j.snb.2013.11.018.
 29. Li, Y.J.; Xie, D.Y.; Pang, X.L.; Yu, X.D.; Yu, T.; Ge, X.T. Highly selective fluorescent sensing for fluoride based on a covalently bonded europium mesoporous hybrid material. *Sensors and Actuators B-Chemical* **2016**, *227*, 660-667, doi:10.1016/j.snb.2016.01.047.
 30. Li, W.K.; Ding, Y.Z.; Feng, J.T.; Ma, Z.Q. A novel luminescent dual-ligands europium(III) complex prepared for acetaldehyde sensitive detection. *Sensors and Actuators B-Chemical* **2020**, *306*, doi:10.1016/j.snb.2019.127542.
 31. Armelao, L.; Quici, S.; Barigelletti, F.; Accorsi, G.; Bottaro, G.; Cavazzini, M.; Tondello, E. Design of luminescent lanthanide complexes: From molecules to

- highly efficient photo-emitting materials. *Coordination Chemistry Reviews* **2010**, *254*, 487-505, doi:10.1016/j.ccr.2009.07.025.
32. Utochnikova, V.V.; Vatsadze, I.A.; Tsymbarenko, D.M.; Goloveshkin, A.S.; Vatsadze, S.Z. Europium complexes with dinitropyrazole: unusual luminescence thermal behavior and irreversible temperature sensing. *Phys Chem Chem Phys* **2021**, *23*, 25480-25484, doi:10.1039/d1cp03924e.
 33. Xia, T.; Shao, Z.; Yan, X.; Liu, M.; Yu, L.; Wan, Y.; Chang, D.; Zhang, J.; Zhao, D. Tailoring the triplet level of isomorphous Eu/Tb mixed MOFs for sensitive temperature sensing. *Chem Commun (Camb)* **2021**, *57*, 3143-3146, doi:10.1039/d1cc00297j.
 34. Khudoleeva, V.; Tcelykh, L.; Kovalenko, A.; Kalyakina, A.; Goloveshkin, A.; Lepnev, L.; Utochnikova, V. Terbium-europium fluorides surface modified with benzoate and terephthalate anions for temperature sensing: Does sensitivity depend on the ligand? *Journal of Luminescence* **2018**, *201*, 500-508, doi:10.1016/j.jlumin.2018.05.002.
 35. Brites, C.D.S.; Balabhadra, S.; Carlos, L.D. Lanthanide-Based Thermometers: At the Cutting-Edge of Luminescence Thermometry. *Advanced Optical Materials* **2019**, *7*, doi:10.1002/adom.201801239.
 36. Outis, M.; Laia, C.A.T.; Oliveira, M.C.; Monteiro, B.; Pereira, C.C.L. A Europium(III) Complex with an Unusual Anion-Cation Interaction: A Luminescent Molecular Thermometer for Ratiometric Temperature Sensing. *Chempluschem* **2020**, *85*, 580-586, doi:10.1002/cplu.202000034.
 37. Sekiguchi, T.; Sotoma, S.; Harada, Y. Fluorescent nanodiamonds as a robust temperature sensor inside a single cell. *Biophys Physicobiol* **2018**, *15*, 229-234, doi:10.2142/biophysico.15.0_229.
 38. Takayama, Y.; Kusamori, K.; Nishikawa, M. Click Chemistry as a Tool for Cell Engineering and Drug Delivery. *Molecules* **2019**, *24*, doi:10.3390/molecules24010172.
 39. Kolb, H.C.; Finn, M.G.; Sharpless, K.B. Click Chemistry: Diverse Chemical Function from a Few Good Reactions. *Angew Chem Int Ed Engl* **2001**, *40*, 2004-2021, doi:10.1002/1521-3773(20010601)40:11<2004::aid-anie2004>3.3.co;2-x.
 40. Hein, C.D.; Liu, X.M.; Wang, D. Click chemistry, a powerful tool for pharmaceutical sciences. *Pharm Res* **2008**, *25*, 2216-2230, doi:10.1007/s11095-008-9616-1.
 41. Agrahari, A.K.; Bose, P.; Jaiswal, M.K.; Rajkhowa, S.; Singh, A.S.; Hotha, S.; Mishra, N.; Tiwari, V.K. Cu(I)-Catalyzed Click Chemistry in Glycoscience and Their Diverse Applications. *Chem Rev* **2021**, *121*, 7638-7956, doi:10.1021/acs.chemrev.0c00920.
 42. Worell, B.T.; Malik, J.A.; Fokin, V.V. *Science*. **2013**, *340*, 457-460, doi:10.1126/science.1229506.
 43. Farrer, N.J.; Griffith, D.M. Exploiting azide-alkyne click chemistry in the synthesis, tracking and targeting of platinum anticancer complexes. *Curr Opin Chem Biol* **2020**, *55*, 59-68, doi:10.1016/j.cbpa.2019.12.001.
 44. Jiang, X.; Hao, X.; Jing, L.; Wu, G.; Kang, D.; Liu, X.; Zhan, P. Recent applications of click chemistry in drug discovery. *Expert Opin Drug Discov* **2019**, *14*, 779-789, doi:10.1080/17460441.2019.1614910.
 45. Yoon, H.Y.; Koo, H.; Kim, K.; Kwon, I.C. Molecular imaging based on metabolic glycoengineering and bioorthogonal click chemistry. *Biomaterials* **2017**, *132*, 28-36, doi:10.1016/j.biomaterials.2017.04.003.

46. Phetsang, W.; Pelington, R.; Butler, M.S.; Sanjaya, K.C.; Pitt, M.E.; Kaeslin, G.; Cooper, M.A.; Blaskovich, M.A.T. Fluorescent Trimethoprim Conjugate Probes To Assess Drug Accumulation in Wild Type and Mutant Escherichia coli. *Acs Infectious Diseases* **2016**, *2*, 688-701, doi:10.1021/acsinfecdis.6b00080.
47. Yang, Y.Q.; Gao, H.Y.; Sun, X.Y.; Sun, Y.H.; Qiu, Y.P.; Weng, Q.J.; Rao, Y. Global PROTAC Toolbox for Degrading BCR-ABL Overcomes Drug-Resistant Mutants and Adverse Effects. *Journal of Medicinal Chemistry* **2020**, *63*, 8567-8583, doi:10.1021/acs.jmedchem.0c00967.
48. Zhang, G.F.; Wang, Y.; Wen, X.; Ding, C.R.; Li, Y. Dual-functional click-triazole: a metal chelator and immobilization linker for the construction of a heterogeneous palladium catalyst and its application for the aerobic oxidation of alcohols. *Chemical Communications* **2012**, *48*, 2979-2981, doi:10.1039/c2cc18023e.
49. Pajk, S.; Zivec, M.; Sink, R.; Sosic, I.; Neu, M.; Chung, C.W.; Martinez-Hoyos, M.; Perez-Herran, E.; Alvarez-Gomez, D.; Alvarez-Ruiz, E.; et al. New direct inhibitors of InhA with antimycobacterial activity based on a tetrahydropyran scaffold. *European Journal of Medicinal Chemistry* **2016**, *112*, 252-257, doi:10.1016/j.ejmech.2016.02.008.
50. VEK, N. Sinteza in karakterizacija novih anionskih fluoroforov iz družine polimetinov. *Diploma thesis* **2019**.
51. Gungor, S.A.; Tumer, M.; Kose, M.; Erkan, S. Benzaldehyde derivatives with functional propargyl groups as alpha-glucosidase inhibitors. *Journal of Molecular Structure* **2020**, *1206*, doi:10.1016/j.molstruc.2020.127780.
52. Liu, G.H.; Shi, G.H.; Sheng, H.Y.; Jiang, Y.Y.; Liang, H.J.; Liu, S.Y. Doubly Caged Linker for AND-Type Fluorogenic Construction of Protein/Antibody Bioconjugates and In Situ Quantification. *Angewandte Chemie-International Edition* **2017**, *56*, 8686-8691, doi:10.1002/anie.201702748.
53. Clough, S.; Gupton, J.; Ligali, A.; Roberts, M.; Driscoll, D.; Annett, S.; Hewitt, A.; Hudson, M.; Jackson, E.; Miller, R.; et al. Reactions of (Z)-3-aryl-3-chloropropenals with nucleophiles: stereoselective formation of (E)-vinylogous esters, (E)-vinylogous amides, and vinamidinium salts. *Tetrahedron* **2005**, *61*, 7554-7561, doi:10.1016/j.tet.2005.05.061.
54. Belov, V.N.; Bossi, M.L.; Folling, J.; Boyarskiy, V.P.; Hell, S.W. Rhodamine Spiroamides for Multicolor Single-Molecule Switching Fluorescent Nanoscopy. *Chemistry-a European Journal* **2009**, *15*, 10762-10776, doi:10.1002/chem.200901333.
55. Manahelohe, G.M.; Potapov, A.Y.; Shikhaliev, K.S. Synthesis of new hydroquinolinecarbaldehydes. *Russian Chemical Bulletin* **2016**, *65*, 1145-1147, doi:10.1007/s11172-016-1427-7.
56. Kaur, J.; Saxena, M.; Rishi, N. An Overview of Recent Advances in Biomedical Applications of Click Chemistry. *Bioconjug Chem* **2021**, *32*, 1455-1471, doi:10.1021/acs.bioconjchem.1c00247.
57. Croissant, J.G.; Mauriello-Jimenez, C.; Maynadier, M.; Cattoen, X.; Man, M.W.C.; Raehm, L.; Mongin, O.; Blanchard-Desce, M.; Garcia, M.; Gary-Bobo, M.; et al. Synthesis of disulfide-based biodegradable bridged silsesquioxane nanoparticles for two-photon imaging and therapy of cancer cells. *Chemical Communications* **2015**, *51*, 12324-12327, doi:10.1039/c5cc03736k.
58. Sabine, B.; Wolfgang, H. 4-Acyl-5-hydroxy-1-phenyl-3-trifluoromethylpyrazoles: Synthesis and NMR Spectral Investigations. **2006**, *68*, 1825-1836, doi:10.3987/COM-05-10502.

59. Hassan, M.Z.; Khan, S.A.; Amir, M. Design, synthesis and evaluation of N-(substituted benzothiazol-2-yl)amides as anticonvulsant and neuroprotective. *European Journal of Medicinal Chemistry* **2012**, *58*, 206-213, doi:10.1016/j.ejmech.2012.10.002.